Accepted Manuscript

Asymmetric 1,5-diarylpenta-1,4-dien-3-ones: Antiproliferative activity in prostate epithelial cell models and pharmacokinetic studies

Xiaojie Zhang, Shanchun Guo, Chengsheng Chen, German Ruiz Perez, Changde Zhang, Manee Patanapongpibul, Nithya Subrahmanyam, Rubing Wang, Joshua Keith, Guanglin Chen, Yan Dong, Qiang Zhang, Qiu Zhong, Shilong Zheng, Guangdi Wang, Qiao-Hong Chen

PII: S0223-5234(17)30433-6

DOI: 10.1016/j.ejmech.2017.05.062

Reference: EJMECH 9492

To appear in: *European Journal of Medicinal Chemistry*

Received Date: 6 March 2017

Revised Date: 18 May 2017

Accepted Date: 31 May 2017

Please cite this article as: X. Zhang, S. Guo, C. Chen, G.R. Perez, C. Zhang, M. Patanapongpibul, N. Subrahmanyam, R. Wang, J. Keith, G. Chen, Y. Dong, Q. Zhang, Q. Zhong, S. Zheng, G. Wang, Q.-H. Chen, Asymmetric 1,5-diarylpenta-1,4-dien-3-ones: Antiproliferative activity in prostate epithelial cell models and pharmacokinetic studies, *European Journal of Medicinal Chemistry* (2017), doi: 10.1016/j.ejmech.2017.05.062.

Table of Contents Graphic

Asymmetric 1,5-Diarylpenta-1,4-dien-3-ones: Antiproliferative Activity in Prostate Epithelial Cell Models and Pharmacokinetic Studies, Xiaojie Zhang, Shanchun Guo, Chengsheng Chen, German Ruiz Perez, Changde Zhang, Manee Patanapongpibul, Nithya Subrahmanyam, Rubing Wang, Joshua Keith, Guanglin Chen, Yan Dong, Qiang Zhang, Qiu Zhong, Shilong Zheng, Guangdi Wang, and Qiao-Hong Chen

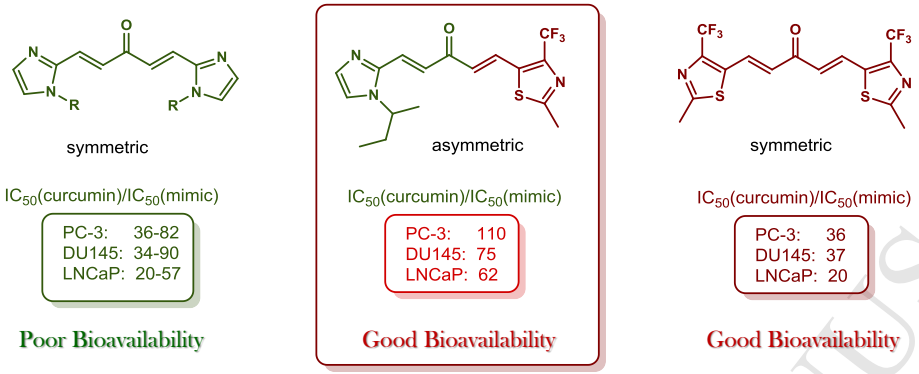

Asymmetric 1,5-Diarylpenta-1,4-dien-3-ones: Antiproliferative Activity in Prostate Epithelial Cell Models and Pharmacokinetic Studies

Xiaojie Zhang[a], Shanchun Guo[b,c], Chengsheng Chen[a], German Ruiz Perez[a], Changde Zhang[b,c], Manee Patanapongpibul[a], Nithya Subrahmanyam[a], Rubing Wang[a], Joshua Keith[a], Guanglin Chen[a], Yan Dong[d], Qiang Zhang[b,c], Qiu Zhong[b,c], Shilong Zheng[b,c], Guangdi Wang[b,c], and Qiao-Hong Chen[a,*]

[a]Department of Chemistry, California State University, Fresno, 2555 E. San Ramon Avenue, M/S SB70, Fresno, CA 93740, USA

[b]Department of Chemistry and [c]RCMI Cancer Research Center, Xavier University of Louisiana, 1 Drexel Drive, New Orleans, LA 70125, USA

[d]Department of Structural and Cellular Biology, Tulane University School of Medicine, New Orleans, LA 70112, USA

ABSTRACT: To further engineer dienones with optimal combinations of potency and bioavailability, thirty-four asymmetric 1,5-diarylpenta-1,4-dien-3-ones (**25**-**58**) have been designed and synthesized for the evaluation of their *in vitro* anti-proliferative activity in three human prostate cancer cell lines and one non-neoplastic prostate epithelial cell line. All these asymmetric dienones are sufficiently more potent than curcumin and their corresponding symmetric counterparts. The optimal dienone **58**, with IC_{50} values in the range of 0.03-0.12 μM, is 636-, 219-, and 454-fold more potent than curcumin in three prostate cancer cell models. Dienones **28** and **49** emerged as the most promising asymmetric dienones that warrant further preclinical studies. The two lead compounds demonstrated substantially improved potency in cell models and superior bioavailability in rats, while exhibiting no acute toxicity in the animals at the dose of 10 mg/kg. Dienones **28** and **46** can induce PC-3 cell cycle regulation at the G_0/G_1 phase. However, dienone **28** induces PC-3 cell death in a different way from **46** even though they share the same scaffold, indicating that terminal heteroaromatic rings are critical to the action of mechanism for each specific dienone.

Key words: 1,5-diheteroarylpenta-1,4-dien-3-one, prostate cancer, cell proliferation, pharmacokinetic study, cell apoptosis

Corresponding author.

*E-mail: qchen@csufresno.edu. Phone: (+1)5592782394. Fax: (+1)5592784402.

1. Introduction

Curcumin (**1**), a pleiotropic diarylheptanoid, is the major chemical component contributing to the diverse bioactivities of turmeric (the rhizomes of *Curcuma longa* L.) [1]. The potential of curcumin in treating prostate cancer has been intensively investigated since 2000 when its capability in suppressing prostate cancer cell proliferation was first revealed by Dorai and co-workers [2-4]. To address its key weaknesses as a drug candidate, a plethora of research efforts have been devoted to the development of its analogues with improved potency and/or bioavailability [3,5]. Monoketone curcumin mimics, in which the metabolically unstable diketone moiety in curcumin is substituted with a monoketone, have been demonstrated as a group of promising anti-cancer agents with 10-20 times improved *in vitro* potency relative to curcumin [3,5]. Our laboratory has systematically investigated the effect of central monoketone-containing linker and terminal rings on the *in vitro* potency of the monoketone curcumin mimics in prostate cancer cell models [6-9]. Our previous findings have revealed that terminal basic nitrogen-containing heteroaromatic rings are obviously beneficial to the enhanced cytotoxic and anti-proliferative potency and that the 1,5-diheteroarylpenta-1,4-dien-3-one is the most promising class of curcumin-based anti-prostate cancer agents, with the most potent compounds being over 100 folds more potent than curcumin against prostate cancer cell lines [6,7]. Most monoketone curcumin mimics are symmetric with two identical terminal aromatic rings, but a few of recent reports suggest that asymmetric monoketone curcumin mimics might exhibit more desirable biological profile as compared to the corresponding symmetric counterparts [10,11]. All 1,5-diheteroarylpenta-1,4-dien-3-ones previously reported by us are symmetric with two identical terminal nitrogen-containing heteroaromatic rings [7], but we have noticed from our previous data that different terminal heteroaromatic rings can bring in varied benefits to the scaffold of 1,5-diheteroarylpenta-1,4-dien-3-one. For example, 1-alkyl-1*H*-imidazol-2-yl moiety in analogues **2**-**4** and 1-alkyl-1*H*-benzo[*d*]imidazole-2-yl moiety in analogues **5**-**6** (Figure 1) are beneficial to the optimal potency of these compounds, whereas 1-alkyl-1*H*-imidazol-2-yl moiety in analogue **3** affords little enhancement in its pharmacokinetic profile. On the other hand, 2-methyl-4-(trifluoromethyl)thiazol-5-yl bestows analogue **7** with an attractive *in vivo* pharmacokinetic profile but only with a moderate increase in potency [7]. These data prompted us to explore a new group of asymmetric 1,5-diheteroarylpenta-1,4-dien-3-ones (**25**-**58**) with the hope of integrating optimal potency and pharmacokinetic profile by incorporating two different heteroaromatic rings into a single curcumin dienone mimic.

The standard of care for prostate cancer has been androgen deprivation therapy (ADT) to block androgen-dependent prostate cancer growth. However, after varying duration of progression free period, most late stage prostate cancers eventually progress to castration-resistant tumors that are no longer responsive to ADT. Further treatment with CYP17A1 inhibitors such as abiraterone or AR antagonists such as enzalutamide has clinically proven to prolong patient survival but the disease remains incurable beyond this stage. Expression of truncated AR variant proteins via AR alternative splicing emerged as an important mechanism of abiraterone and enzalutamide resistance in prostate cancer. Therefore, new anticancer agents that can overcome resistance to current CRPC regimens are highly desirable. To this end, we also evaluated the activities of selected asymmetric curcumin mimics in three prostate cancer cell lines that harbor AR splicing variants and are resistant to enzalutamide treatment.

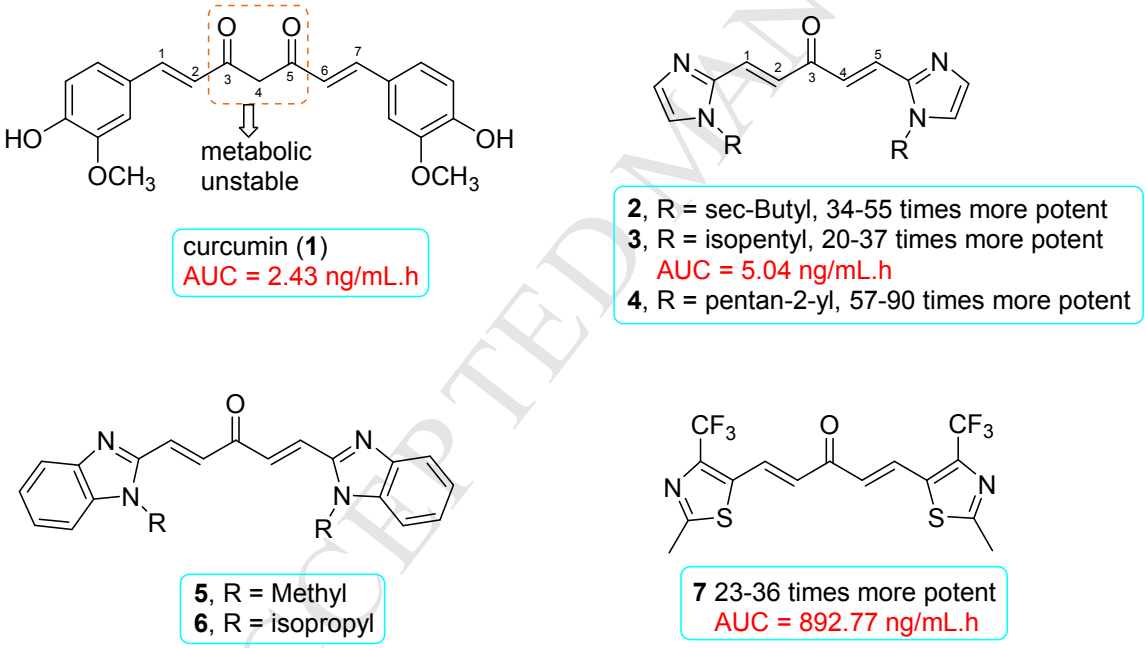

Fig. 1. Structures, antiproliferative potency, and pharmacokinetic profiles of curcumin and symmetric 1,5-diheteroarylpenta-1,4-dien-3-ones (**2**-**7**) [7]

2. Results and Discussion

2.1 Chemistry

The desired thirty-four asymmetric 1,5-diheteroarylpenta-1,4-dien-3-ones (**25**-**58**) have been synthesized through two sequential Horner-Wadsworth-Emmons reactions of 1,3-bis(diethylphosphonato)acetone (**9**) with the appropriate aromatic carbadehyde (**8**) (Scheme 1). 1-Alkyl-1*H*-imidazole-2-carbaldehydes and 1-alkyl-1*H*-benzo[d]imidazole-2-carbaldehydes were synthesized according to the procedure illustrated in the literature [7,12]. All other aromatic carbaldehydes were obtained from commercial sources. In the case of preparing fifteen (*E*)-diethyl(2-oxo-4-heteroaryl-but-3-en-1-yl)phosphonates (**10**-**24**) as the intermediates through the Horner-Wadsworth-Emmons reaction, 1 equivalent of the appropriate carbaldehye was added slowly to the reaction mixture of 1 equivalent of 1,3-bis(diethylphosphonato)acetone (**9**) and potassium carbonate in ethanol and water (0.1 M). This strategy was implemented to reduce the formation of symmetric 1,5-diheteroarylpenta-1,4-dien-3-ones.

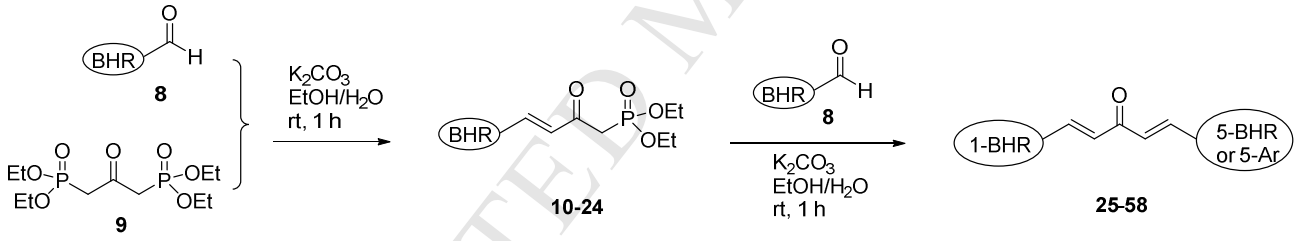

Note: BHR: Basic nitrogen containing heteroaromatic ring.

For the structures of phosphonates **10**-**24**, refer to Table 1.

For the structures of dienones **25**-**58**, refer to Table 2.

Scheme 1. Synthesis of asymmetric 1,5-diheteroarylpenta-1,4-dien-3-ones (**25**-**58**)

Table 1
Structures for (*E*)-diethyl(2-oxo-4-heteroaryl-but-3-en-1-yl)phosphonates **10**-**24**

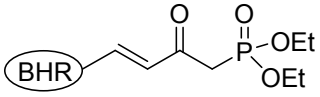

BHR	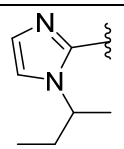	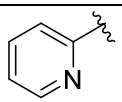	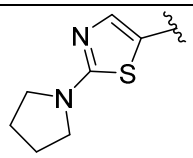	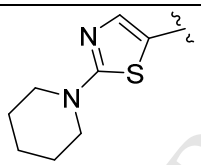	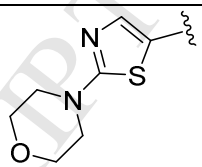
compd	**10**	**11**	**12**	**13**	**14**
BHR	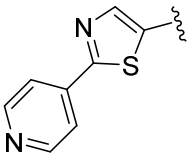	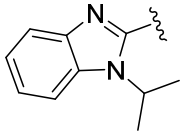	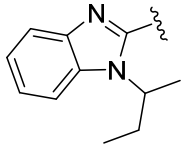	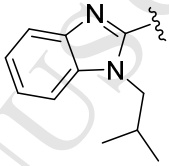	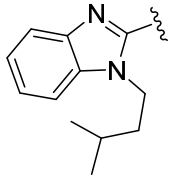
compd	**15**	**16**	**17**	**18**	**19**
BHR	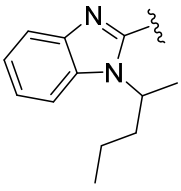	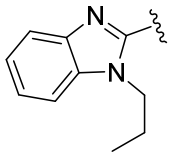	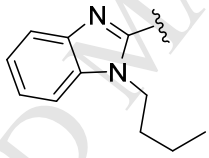	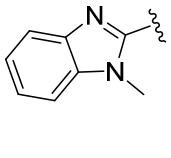	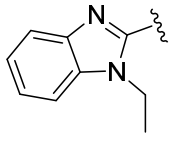
compd	**20**	**21**	**22**	**23**	**24**

Table 2
Structures for asymmetric 1,5-diarylpenta-1,4-dien-3-ones (**25**-**58**)

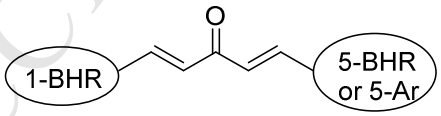

Compd	1-BHR	5-BHR or 5-AR	Compd	1-BHR	5-BHR or 5-AR
25	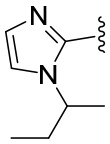	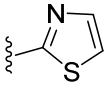	**26**	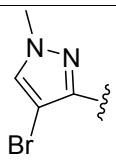	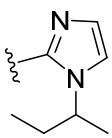

27

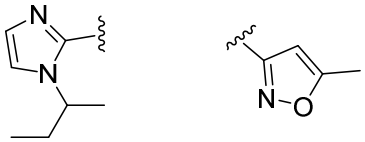

28

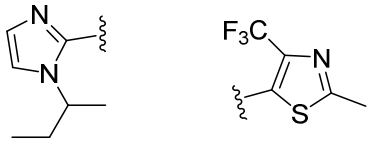

29

30

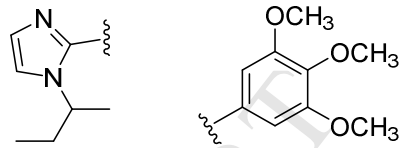

31

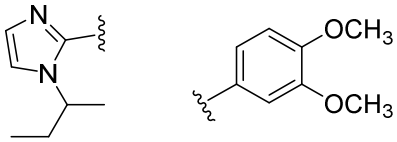

32

33

34

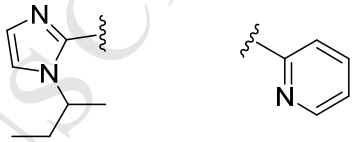

35

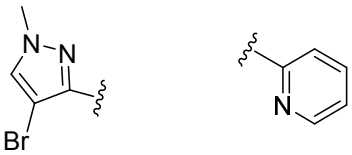

36

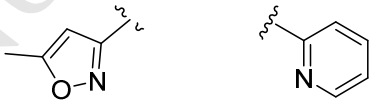

37

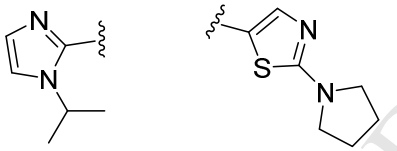

38

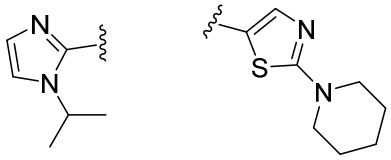

39

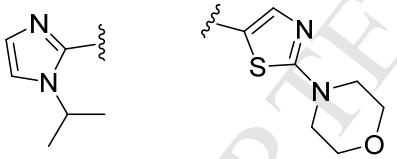

40

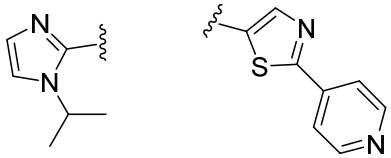

41

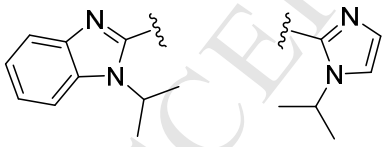

42

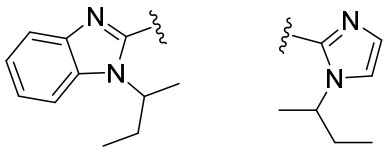

43

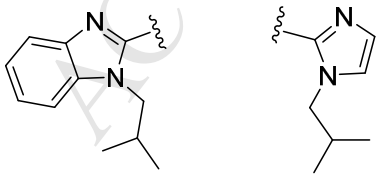

44

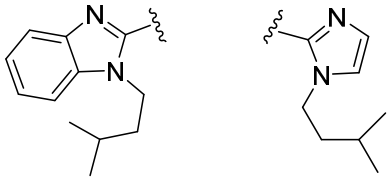

45

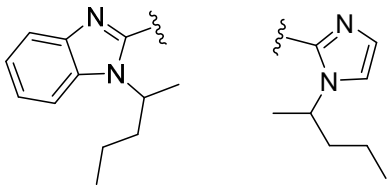

46

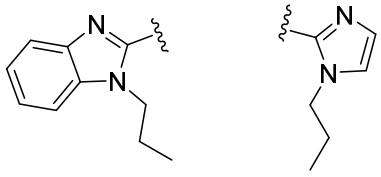

47	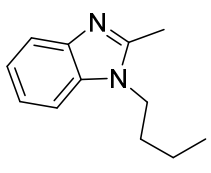	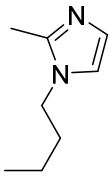	**48**	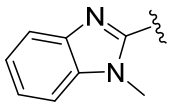	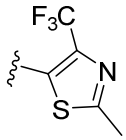
49	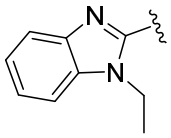	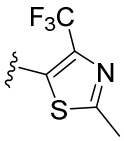	**50**	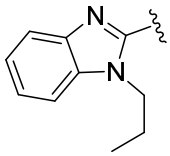	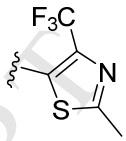
51	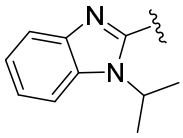	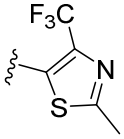	**52**	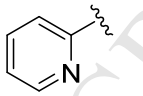	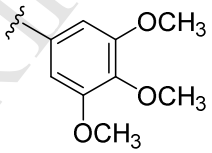
53	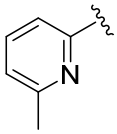	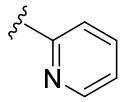	**54**	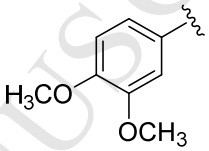	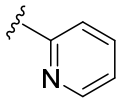
55	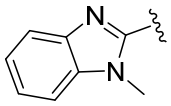	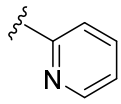	**56**	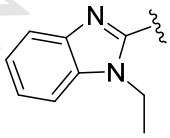	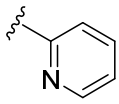
57	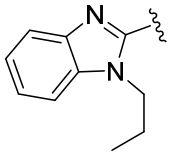	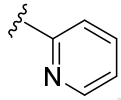	**58**	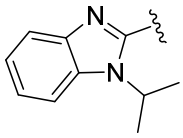	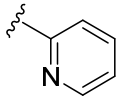

2.2 Antiproliferative Activity towards Prostate Cancer Cell Lines

The *in vitro* anti-proliferative activity of the thirty-four asymmetric 1,5-diheteroarylpenta-1,4-dien-3-ones (**25**-**58**) against both androgen-sensitive and androgen-insensitive prostate cancer cell lines (LNCaP, DU145, and PC-3) were assessed by WST-1 cell proliferation assay according to the procedure as described in the Experimental Section. Curcumin was used as a positive control for comparison and the anti-proliferative potency of each test dienone was represented as IC_{50} values. As shown in Table 3, all the asymmetric dienones exhibit much greater potency than curcumin in suppressing prostate cancer cell proliferation. Their IC_{50} values towards PC-3, DU145, and LNCaP human prostate cancer cell line are in the ranges of 0.04-6.86 μM, 0.12-3.68 μM, and 0.03-4.05 μM,

respectively. The optimal dienone **58** with IC_{50} values in the range of 0.03-0.12 μM is 636-, 219-, and 454-fold more potent than curcumin in three prostate cancer cell models.

The structure-antiproliferative activity relationships of the asymmetric 1,5-diheteroarylpenta-1,4-dien-3-ones can be summarized as below:

- All thirty-four asymmetric 1,5-diheteroarylpenta-1,4-dien-3-ones exhibit far greater potency towards three human prostate cancer cell lines (Table 3) than curcumin, implying that asymmetric (1*E*, 4*E*)-1,5-diheteroarylpenta-1,4-dien-3-one is an optimal scaffold for curcumin mimics with substantially improved potency in inhibiting prostate cancer cell proliferation.

- Asymmetric 1,5-diheteroarylpenta-1,4-dien-3-ones (**25**-**58**) are significantly more potent than their symmetric counterparts reported previously by us [7]. For example, (1*E*,4*E*)-1,5-bis(1-isopropyl-1*H*-benzo[*d*]imidazol-2-yl)penta-1,4-dien-3-one (**6**, symmetric) is 30-111 times more potent [7] and (1*E*,4*E*)-1,5-di(pyridin-2-yl)penta-1,4-dien-3-one (symmetric) is 15-60 folds more potent [6] than curcumin towards three prostate cancer cell lines; in contrast, the asymmetric version (dienone **58**) with pyridine-2-yl and 1-isopropyl-1*H*-benzo[*d*]imidazole-2-yl moieties is 219-636 folds more potent than curcumin.

- The following four pairs of heteroaromatic rings serve as the optimal combinations of the terminal rings for the promising potency: i) 1-alkyl-1*H*-imidazol-2-yl and 2-methyl-4-(trifluoromethyl)thiazol-5-yl moieties in dienone **28**, ii) 1-alkyl-1*H*-imidazol-2-yl and 1-alkyl-1*H*-benzo[*d*]imidazole-2-yl moieties in dienones **41**-**47**, iii) 1-alkyl-1*H*-benzo[*d*]imidazole-2-yl and 2-methyl-4-(trifluoromethyl)thiazol-5-yl moieties in dienone **49**, and iv) 1-alkyl-1*H*-benzo[*d*]imidazole-2-yl and pyridine-2-yl moieties in dienones **56**-**58**.

Table 3
Anti-proliferative activity of the asymmetric 1,5-diheteroarylpenta-1,4-dien-3-ones (**25**-**58**) toward three prostate cancer cell lines

Compd	IC_{50} (μM)[a]			IC_{50} (curcumin)/IC_{50}(dienone)		
	PC-3[b]	DU145[c]	LNCaP[d]	PC-3[b]	DU145[c]	LNCaP[d]
Curcumin	25.43 ± 2.15	26.23 ± 0.65	13.61 ± 2.69	1	1	1
25	0.39 ± 0.08	0.42 ± 0.09	0.17 ± 0.02	64	62	80

26	0.33 ± 0.02	0.28 ± 0.04	0.31 ± 0.01	76	94	44
27	0.31 ± 0.03	0.53 ± 0.04	0.24 ± 0.04	82	50	57
28	0.23 ± 0.02	0.35 ± 0.04	0.22 ± 0.05	110	75	62
29	0.37 ± 0.02	0.75 ± 0.03	0.24 ± 0.04	69	35	57
30	0.72 ± 0.01	0.67 ± 0.02	0.66 ± 0.04	35	39	21
31	1.33 ± 0.20	0.85 ± 0.04	0.91 ± 0.08	19	31	15
32	0.26 ± 0.02	0.29 ± 0.03	0.26 ± 0.02	98	90	52
33	0.55 ± 0.05	1.13 ± 0.12	0.45 ± 0.07	46	23	30
34	0.30 ± 0.04	0.34 ± 0.05	0.24 ± 0.02	85	77	57
35	0.31 ± 0.03	0.50 ± 0.03	0.22 ± 0.01	82	53	62
36	0.45 ± 0.04	0.70 ± 0.10	0.31 ± 0.11	57	38	44
37	6.86 ± 0.37	3.68 ± 0.08	4.05 ± 0.76	4	7	3
38	3.40 ± 0.21	2.55 ± 0.23	2.17 ± 0.19	8	10	6
39	2.27 ± 0.12	1.32 ± 0.27	1.41 ± 0.13	11	20	10
40	0.80 ± 0.04	0.66 ± 0.16	0.54 ± 0.05	32	40	25
41	0.18 ± 0.01	0.13 ± 0.10	0.26 ± 0.07	141	138	52
42	0.24 ± 0.02	0.35 ± 0.05	0.33 ± 0.05	106	75	41
43	0.20 ± 0.05	0.37 ± 0.12	0.56 ± 0.05	127	71	24
44	0.21 ± 0.04	0.77 ± 0.20	0.93 ± 0.33	121	34	41
45	0.14 ± 0.04	0.28 ± 0.04	0.37 ± 0.14	182	94	37
46	0.10 ± 0.01	0.22 ± 0.03	0.22 ± 0.11	254	119	62
47	0.19 ± 0.04	0.31 ± 0.08	0.40 ± 0.03	134	85	34

48	0.48 ± 0.02	0.78 ± 0.06	0.34 ± 0.09	53	34	40
49	0.23 ± 0.00	0.50 ± 0.02	0.25 ± 0.03	110	53	54
50	0.55 ± 0.03	0.84 ± 0.14	0.46 ± 0.07	46	31	30
51	0.34 ± 0.05	0.57 ± 0.04	0.30 ± 0.19	75	46	45
52	0.84 ± 0.03	0.83 ± 0.09	0.40 ± 0.02	30	32	34
53	0.54 ± 0.04	0.63 ±0.06	0.30 ± 0.07	47	42	45
54	1.70 ± 0.20	2.05 ± 0.15	1.76 ± 0.15	15	13	8
55	0.56 ± 0.05	0.68 ± 0.27	0.18 ± 0.04	45	39	76
56	0.23 ± 0.02	0.46 ± 0.13	0.12 ± 0.05	111	57	113
57	0.25 ± 0.02	0.32 ± 0.05	0.17 ± 0.08	102	82	80
58	0.04 ± 0.01	0.12 ± 0.05	0.03 ± 0.01	636	219	454

[a] IC_{50} is the drug concentration effective in inhibiting 50% of the cell viability measured by WST-1 cell proliferation assay (WST-1) after 3 days exposure. The data were presented as the mean ± standard derivation of the mean.

[b] Human androgen-insensitive prostate cancer cell line

[c] Human androgen-insensitive prostate cancer cell line

[d] Human androgen-sensitive prostate cancer cell line

2.3 Antiproliferative Activity towards PWR-1E Non-neoplastic Human Prostate Epithelial Cell Line

Fifteen dienones (**25**-**28**, **32**, **34**-**35**, **41**, **45**-**46**, **49**, **51**, and **56**-**58**) were selected as the representatives of different subgroups for further evaluation of their ability in inhibiting PWR-1E benign human prostatic epithelial cell proliferation. **25**-**28** are the optimal dienones with two different five-membered heteroaromatic rings; **32**, **34**, and **35** are the representatives of the dienones with one five-membered and one six-membered heteroaromatic rings; **41**, **45**-**46**, **49**, and **51** are those good examples with bicyclic 1-alkyl-1*H*-benzo[*d*]imidazole-2-yl as one terminal ring and a five-membered heteromatic as another terminal ring; and **56**-**58** represent the subgroup having one bicyclic 1-alkyl-1*H*-benzo[*d*]imidazole-2-yl as one terminal ring and one six-membered heteromatic as the other terminal ring. PWR-1E human prostatic epithelial cell line expresses prostate specific antigen (PSA) and androgen receptor (AR) and mimics normal growth and differentiation responses to androgen [13]. The

PWR-1E cell line was originally isolated from a non-malignant prostate with mild hyperplasia and immortalized by adenovirul 12/Simian 40. Curcumin was used as a positive control as curcumin's general human safety profile has been validated by clinical trials [4,14] and animal studies [15]. The apoptotic cell death pathway in both normal human primary prostate epithelial cells and androgen-sensitive human prostate cancer cells could be triggered by androgen deprivation [16]. In this study, we observed the IC_{50} values for curcumin are 8.55 μM for PWR-1E cells and 13.61 μM for LNCaP cells, suggesting no differential responses to LNCaP and PWR-1E cells. This is reasonable considering that curcumin can downregulate the expression and activity of AR and PSA in LNCaP prostate cancer cells [17] and that both LNCaP prostate cancer cells and PWR-1E non-neoplastic prostate epithelial cell lines express androgen receptor and androgen specific antigen. As shown in Table 4, the asymmetric dienones have 63- to 885-fold greater potency in suppressing PWR-1E benign prostate cell proliferation, as compared with curcumin. The asymmetric 1,5-diheteroarylpenta-1,4-dien-3-ones (**25**, **26**-**28**, **32**, **34**-**35**) having five-membered and six-membered heteroaromatic rings as their terminal rings display approximately equivalent potency towards the PWR-1E non-neoplastic prostate epithelial cell line and the three human prostate cancer cell lines; while the asymmetric 1,5-diheteroarylpenta-1,4-dien-3-ones (**41**, **45**-**46**, **49**, **51**, and **56**-**58)** possessing a bicyclic 1-alkyl-1*H*-benzo[*d*]imidazole-2-yl as one terminal ring exhibit substantially higher anti-proliferative potency against the PWR-1E non-neoplastic prostate epithelial cell line than three human prostate cancer cell lines.

Table 4

Anti-proliferative activity of selected asymmetric 1,5-diheteroarylpenta-1,4-dien-3-ones toward PWR-1E prostate epithelial cells that express AR and PSA.

Compd	IC_{50} (μM)	IC_{50} (curcumin)/IC_{50}(dienone)
Curcumin	8.85 ± 0.70	1
25	0.14 ± 0.03	63
26	0.14 ± 0.07	63
27	0.11 ± 0.03	81
28	0.11 ± 0.04	81
32	0.13 ± 0.01	68

34	0.17 ± 0.01	52
35	0.10 ± 0.02	89
41	0.03 ± 0.01	293
45	0.04 ± 0.00	221
46	0.02 ± 0.01	443
49	0.08 ± 0.03	111
51	0.05 ± 0.01	177
56	0.04 ± 0.03	221
57	0.02 ± 0.03	443
58	0.01 ± 0.01	885

2.4 In vitro cytotoxicity in enzalutimide-resistant prostate cancer cell models expressing AR splice variants:

To test if the asymmetric curcumin mimics are effective against ligand independent prostate cancer, we treated three cell lines, LNCaP95, VCaP, and 22Rv1 [18,19] with four potent compounds, **28**, **46**, **49**, and **58**. The IC_{50} values, the concentrations for test compounds effective in suppressing 50% of the cell viability, were measured by the trypan blue exclusion assay after 5 days exposure. As shown in Table 5, these four mimics also exhibited impressive cytotoxicity against LNCaP95, VCaP, and 22Rv1 prostate cancer cell lines, with IC_{50} values ranging from 0.22 μM to 1.41 μM.

Table 5
Cytotoxicity of selected asymmetric 1,5-diheteroarylpenta-1,4-dien-3-ones against three ligand independent prostate cancer cell lines expressing AR splice variants.

Compd	IC_{50} (μM)		
	LNCaP95	VCaP	22Rv1
28	0.37	0.35	0.85
46	0.35	1.12	0.22
49	0.38	1.41	0.22
58	0.26	0.64	0.45

2.5. In vivo pharmacokinetic studies and acute toxicity in rat:

The overarching goal of this research is to engineer curcumin mimics with improved potency and bioavailability. To evaluate if the asymmetric curcumin mimics with markedly improved anticancer activities could also possess greater bioavailability, we chose four most promising mimics, **28**, **46**, **49**, and **58**, for pharmacokinetic studies. Among them, dienones **28** and **49** were highly expected to have good bioavailability because they both contain 2-methyl-4-(trifluoromethyl)thizaol-5-yl moiety that has been demonstrated by us to confer analogue **7** with an attractive *in vivo* pharmacokinetic profile in mice [7]. In this study we sought to evaluate the pharmacokinetic profiles for these lead compounds in Sprague Dawley rats, a species that are more suited for bioavailability study. The animals administered with **28**, **46**, **49**, or **58**, via oral gavage at a single dose of 10 mg/kg, and blood samples were collected at 1, 3, 6, and 24 hours after oral administration. Plasma was prepared from the blood samples and was analyzed by HPLC-MS/MS for determination of drug concentrations as described in the Experimental Section. Summarized in Table 6 are the plasma concentrations of **28**, **46**, **49**, and **58** at different sampling time points, which lead to the conclusion that, among the four dienones, compound **46** gains the least improvement in its bioavailability with the peak concentration at 280.9 ng/mL. The relatively poor pharmacokinetic results of (1*E*,4*E*)-1-(1-propyl-1*H*-benzo[*d*]imidazole-2-yl)-5-(1-propyl-1*H*-imidazole-2-yl)penta-1,4-dien-3-one (**46**) are consistent with our previous reports where (1*E*,4*E*)-1,5-bis(1-isopentyl-1*H*-imidazol-2-yl)penta-1,4-dien-3-one (**3**) only showed very little improvement in its peak concentration and AUC value as compared with curcumin.[7] These data collectively suggest that location of 1-alkyl-1*H*-imidazole-2-yl and/ or 1-alkyl-1*H*-benzo[*d*]imidazole-2-yl to both terminal

rings of the dienones resulted in markedly improved anti-proliferative potency, but little enhancement in bioavailability.

Conversely, assignment of a 1-alkyl-1*H*-imidazole-2-yl or 1-alkyl-1*H*-benzo[*d*]imidazole-2-yl moiety as one terminal ring and incorporation of a 2-methyl-4-(trifluoromethyl)thiazol-5-yl or pyridin-2-yl moiety as the other terminal ring lead to the very promising dienones **28**, **49**, and **58** with substantially improved bioavailability, in addition to the great potency. The peak concentration for each of these three dienones (**28**, **49**, and **58**) is 1943.8 ng/mL (5.27 μM), 1225.1 ng/mL (3.25 μM), and 4264.1 ng/mL (13.45 μM), respectively, far exceeding their IC_{50} values ranging from 0.03-0.50 μM in three human prostate cancer cell lines. It is thus reasonable to conclude that the excellent bioavailability of **28**, **49**, and **58**, as demonstrated by their high peak plasma concentration and AUC values, will provide the therapeutic efficacy necessary to block tumor growth.

The acute *in vivo* toxicity in rats indicates that the animals were able to tolerate the dose of 10 mg/kg of dienones **28** and **49** without observed toxicity. However, we noticed that the rats died in about 48 hours and 72 hours, respectively, after orally given **46** or **58** at 10 mg/kg. Therefore, **28** and **49** are more promising asymmetric dienones worthy for further development.

Table 6
24-Hour mouse-plasma concentrations of curcumin, **28**, **46**, **49**, and **58**

Times	Concentration in Plasma (ng/mL)				
	Curcumin[a]	**28**	**46**	**49**	**58**
30 min	0.04				
1 hr	0.33	360.7 ± 3.8	113.9 ± 2.2	112.1 ± 5.9	822.6 ± 62.1
2 hr	0.57				
3 hr		672.4 ± 23.4	196.5 ± 16.7	982.3 ± 44.7	4264.1 ± 185.3
4 hr	0.13				
6 hr		1943.8 ± 47.3	280.9 ± 23.7	1225.1 ± 43.0	456.3 ± 15.2
1 day	0.03	230.3 ± 5.6	86.0 ± 5.9	314.1 ± 1.5	102.7 ± 4.4
t_{max} (hrs)	2	6	6	6	3
C_{max} (ng/mL)	0.57	1943.8 ± 47.3	280.9 ± 23.7	1225.1 ± 1.5	4264.1 ± 185.3
Area under curve (AUC) (ng/mL*h)	2.85	24704.65	4385.55	18314.35	17609.60

[a.] The data for curcumin have been reported in our previous paper [7]

Note: Single oral dose for **28**, **46**, **49**, and **58** is **10 mg/kg** in rats.

Single oral dose for curcumin is **1 mg/kg** in mice.

*2.6.Metabolic profiling of dienones **28** and **49***

A preliminary metabolic transformation study was conducted for dienones **28** and **49** by *in vitro* microsomal incubation experiments to identify major metabolites of these compounds. As shown in Table 7, a total of three major metabolic products of dienone **28** were detected and identified based on chromatographic and mass spectral data collected. All three metabolites, assigned as **28-MO1**, **28-MO2**, and **28-MO3** (Scheme 2), were monohydroxylation products. The polarity of the metabolites with various oxidation sites is consistent with the retention time indicating **28-MO1** is the most polar metabolite followed by **28-MO2** and **28-MO3**. For dienone **49**, only two major metabolic products were observed, **49-MO1** and **49-MO2** (Scheme 3). While the assignment of hydroxylation sites may not be definitive with available analytical information, the mono-oxidation of both parent compounds has been confirmed by their respective high resolution mass spectra (Table 7).

Table 7.
Analytical results of dienones **28**, **49**, and their respective metabolic products.

Compound or metabolite	Retention time (min)	MH^+: Theoretical	Parent ion (observed in positive ion mode)	Mass error (ppm)	Major Fragment ions
28	4.35min	370.1201	370.1195	1.6	121, 246, 314 (M-$CHCH_3CH_2CH_3$)+2H),
28-MO1	3.32min	386.1150	386.1145	1.3	314, 121, 294, 332, 136, 179
28-MO2	3.7min	386.1150	386.1145	1.3	151, 167, 332, 220
28-MO3	3.97min	386.1150	386.1145	1.3	330, 310, 151, 121, 167
49	5.05min	392.1044	392.1039	1.3	199 (M-CHCH-$C_5H_3F_3NS$); 171 (M+H-CHCH-$C_5H_3F_3NS$-CH_2CH_3), 372, 325, 352
49-MO1	4.54min	408.0994	408.0988	1.5	215(M-CHCH-$C_5H_3F_3NS$); 187 (M+H-CHCH-$C_5H_3F_3NS$-CH_2CH_3), 136, 341, 388
49-MO2	4.66min	408.0994	408.0988	1.5	199 (M-CHCH-$C_5H_3F_3NS$-O); 171 (M+H-CHCH-$C_5H_3F_3NS$-CH_2CH_3-O), 388, 215, 171

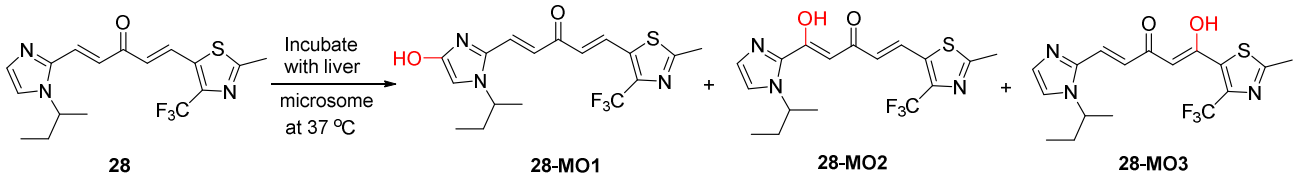

Scheme 2. The metabolites of **28** from incubation with liver microsome

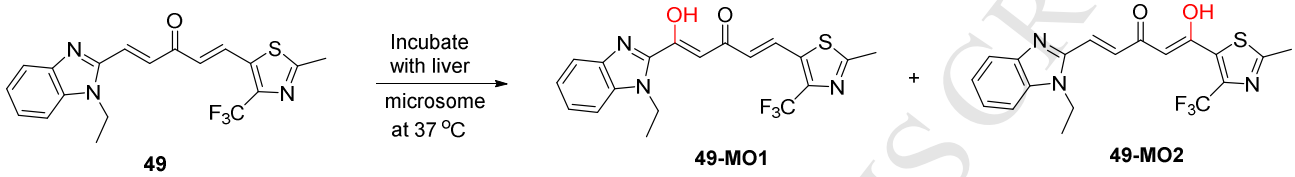

Scheme 3. The metabolites of **49** from incubation with liver microsome

2.7.Cell cycle regulation and cell apoptosis.

Curcumin has been reported to arrest PC-3 cell cycle at the G_1/S phase [20]. The PC-3 cell cycle regulations of dienones **28** and **46** were assessed using flow cytometry analysis with propidium iodide DNA staining. The data illustrated in Figure 2 suggest that both of them induce cell cycle arrest at the G_0/G_1 phase by accumulating PC-3 cell population in the G_0/G_1 phase, while fewer cells were observed in the G_2 phase. Specifically, dienone **46** (4 μM) increases the population of PC-3 cells in the G_0/G_1 phase from 51% and 59% (control cells) at 16 h and 24 h, respectively, to 78% and 76%. The population of cells in the G_2 phase decreases from 25% to 13% at 16 h, and from 24% in control cells to 14% at 24 h. Similarly, treatment of PC-3 cells with dienone **28** (5 μM) led to 14% (at 16 h) and 4% (at 24 h) higher cell population at the G_0/G_1 phase and 10% (at 16 h) and 3% (at 24 h) lower cell population at the G_2 phase, as compared with their control cells.

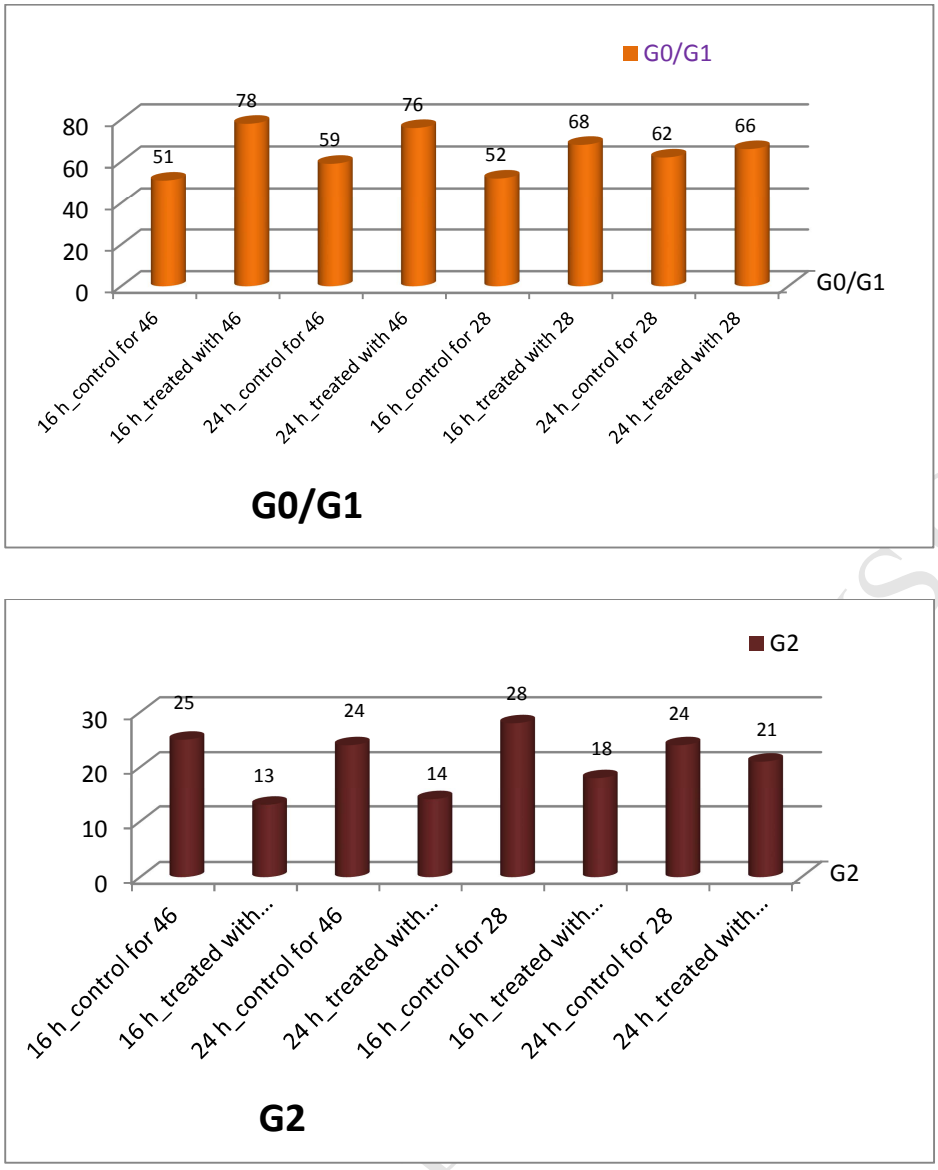

Fig. 2. Cell cycle analysis of PC-3 prostate cancer cells. PC-3 cancer cells were untreated or treated with **28** at 5 µM and **46** at 4 µM, respectively. Cells were harvested after 16 h or 24 h, fixed, stained, and analyzed for DNA content.

The growth suppression of PC-3 prostate cancer cells by curcumin has been demonstrated to be, at least in part, associated with its cell apoptosis activation [2]. The violet excitable dye F2N12S can detect membrane asymmetry changes during apoptosis and SYTOX AADVanced dead cell stain can distinguish the cells with compromised membrane (late apoptotic and necrotic cells) from the viable cells. The F2N12S and SYTOX AADVanced double staining assay in a flow cytometer was employed for the discrimination between early apoptotic PC-3 cells and late apoptotic/necrotic PC-3 cells when

treated with dienones **28** and **46** at the concentrations specified in Figures 3 and 4 for 16 h. Staurosporine, a known apoptotic inducer, was used as positive apoptotic control in all experiments (data not shown). As summarized in Figure 3, dienone **46** can simultaneously activate apoptotic and necrotic cell death in the androgen-insensitive PC-3 prostate cancer cell line after a 16-hour treatment. Specifically, exposure of PC-3 cells to **46** at 4 μM can lead to 22% of PC-3 cells in early phase of apoptosis, as well as 23% late apoptotic/necrotic cells, as compared with control cells; treatment with **46** at 6-15 μM induces 43-52% early apoptotic cells together with 35-47% late apoptotic/necrotic cells. It is worth noting that **28** induces PC-3 cell death in a different way from **46** even though they possess same 1,5-diheteroarylpenta-1,4-dien-3-one scaffold, indicating that terminal heteroaromatic rings might be very important to the action of mechanism for each specific dienone. As shown in Figure 4, incubation of the PC-3 cells with dienone **28** for 16 h induced considerable levels of late apoptotic/necrotic cells rather than early apoptotic cells. For example, 5 μM of dienone **28** can induce 39% late apoptotic/necrotic cells but only 11% early apoptotic cells.

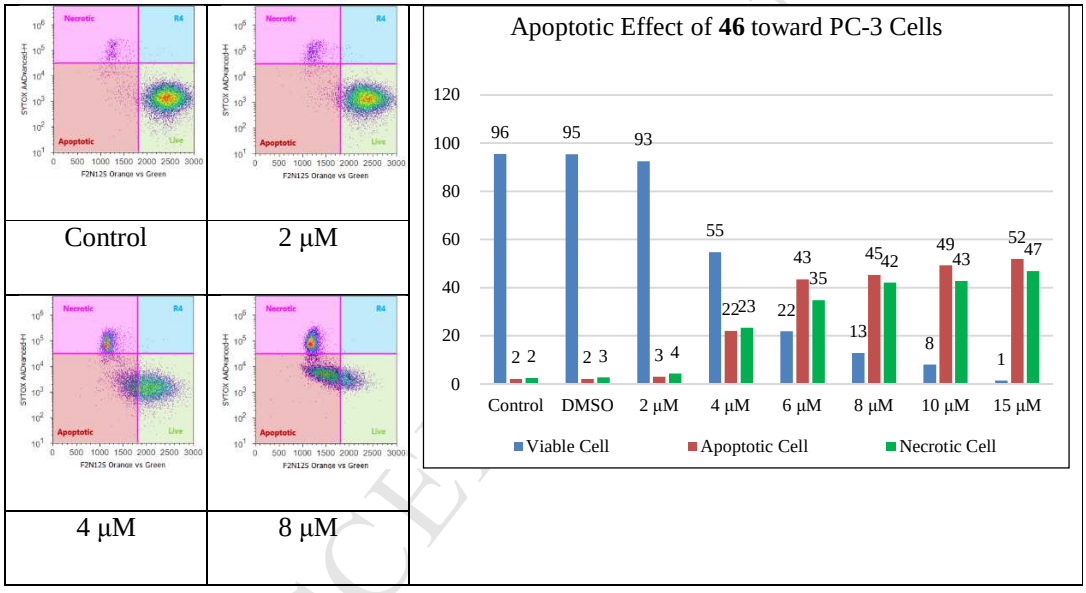

Fig. 3. Evolution of viable, apoptotic, and necrotic PC-3 cells populations in response to **46**.

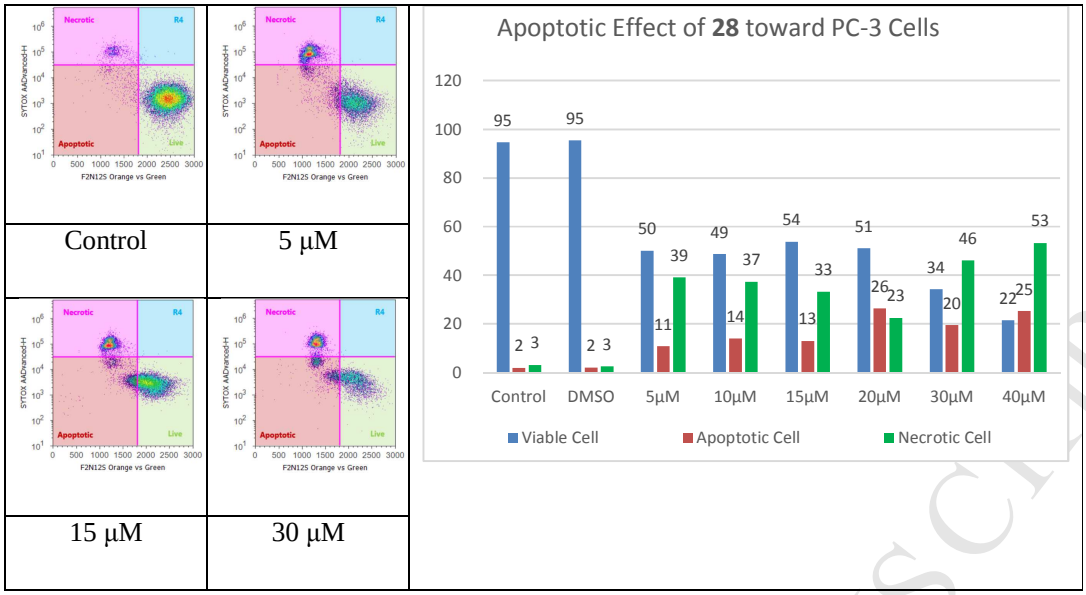

Fig. 4. Evolution of viable, apoptotic, and necrotic PC-3 cells populations in response to **28**.

3. **Conclusion**

To optimize monoketone curcumin mimics as anti-prostate cancer agents, thirty-four asymmetric 1,5-diheteroarylpenta-1,4-dien-3-ones (**25**-**58**) have been designed and synthesized for the evaluation of their in vitro antiproliferative activity in three human prostate cancer cell lines and one human non-neoplastic prostate epithelial cell line. All these asymmetric dienones are sufficiently more potent than curcumin and their corresponding symmetric counterparts. The optimal dienone **58** with IC_{50} values in the range of 0.03-0.12 µM is 636-, 219-, and 454-fold more potent than curcumin in three prostate cancer cell models. However, its in vivo acute toxicity in mice may limit the further development of dienone **58**. Dienones **28** and **49** have been identified as more-promising asymmetric dienones based on their substantially improved potency in cell models and excellent bioavailability in mice, as well as the lack of apparent acute toxicity in the animals at the dose of 10 mg/kg. Importantly, these asymmetric curcumin mimics also demonstrate potent antiproliferative activities against ligand independent, AR-V harboring prostate cancer cells that are resistant to all forms of hormonal therapy. Dienones **28** and **46** can induce PC-3 cell cycle regulation at the G_0/G_1 phase, but dienone **28** induces PC-3 cell death in a different way from **46** even though they possess the same 1,5-diheteroarylpenta-1,4-dien-3-one scaffold, suggesting that the terminal heteroaromatic rings may play a critical role in the underlying mechanism

of action for each specific dienone. The further study on anticancer mechanism of dienone **28** is ongoing.

4. Experimental

4.1 General Procedures

HRMS were obtained on an Orbitrap mass spectrometer with electrospray ionization (ESI). NMR spectra were obtained on a Bruker Fourier 300 spectrometer in $CDCl_3$. The chemical shifts are given in ppm referenced to the respective solvent peak, and coupling constants are reported in Hz. Anhydrous THF and dichloromethane were purified by PureSolv MD 7 Solvent Purification System from Innovative Technologies (MB-SPS-800). All other reagents and solvents were purchased from commercial sources and were used without further purification. Silica gel column chromatography was performed using silica gel (32-63 μm). Preparative thin-layer chromatography (PTLC) separations were carried out on thin layer chromatography plates loaded with silica gel 60 GF254 (EMD Millipore Corporation, MA, USA). Curcumin was synthesized by Claisen-Schmidt condensation of aromatic aldehyde with acetylacetone according to the procedure described in the literature [21]. 1,3-Bis(diethylphosphonato)acetone was synthesized using the procedure illustrated in the literature [22]. The purities of thirty-two out of thirty-four biologically tested compounds are ≥ 95% as determined by HPLC. Specifically, the major peak accounted for ≥ 95% of the combined total peak area when monitored by a Diode Array Detector (DAD) at 325 ± 100 nm. The HPLC analyses were performed on an Agilent Hewlett Packard 1100 Series HPLC DAD system using a 5 μM C_{18} reversed phase column (4.6 mm × 250 mm) and a Diode Array Detector. The purity of two compounds, **37** and **38**, cannot be measured using the above-mentioned conditions. We did not further pursuit their purity because they exhibited the poorest anti-proliferative potency.

*4.2 General procedure for the synthesis of (E)-diethyl(2-oxo-4-aryl-but-3-en-1-yl)phosphonates **10-24*** [8]

A solution of tetraethyl(2-oxopropane-1,3-diyl)bis(phosphonate) (0.4 mmol, 1 equiv.) and potassium carbonate (55 mg, 0.4 mmol, 1 equiv.) in ethanol (1.4 mL) and water (2.1 mL) was stirred at 0^oC for 30 min. The corresponding aromatic carbaldehyde (0.4 mmol, 1 equiv.) was added dropwise to the soltion. The subsequent mixture was stirred at 0 ^oC for 4-10 hours as determined by TLC prior to being quenched with aqueous ammonium chloride solution (15 mL). The mixture was extracted with dichloromethane (10 mL × 3), and the combined dichloromethane layers were dried over anhydrous

magnesium sulfate and concentrated under reduced pressure. The crude product was subjected to PTLC purification using DCM:MeOH (100:10, v/v) as eluent to give the respective phosphonate. The NMR data of phosphonates **11** and **16**-**20** are in consistent with those reported in the literature [8]. The NMR data for other phosphonates (**10**, **12**-**15**, and **21**-**24**) are listed in Supplementary Data.

*4.3 General procedure for the synthesis of asymmetric (1E,4E)-1,5-diheteroarylpenta-1,4-dien-3-ones (**25**-**58**)* [8]

To a solution of the corresponding (*E*)-diethyl(2-oxo-4-aryl-but-3-en-1-yl)phosphonate (0.122 mmoL, 1 equiv.) in ethanol (0.6 mL) and water (0.9 mL) was added potassium carbonate (16 mg, 0.122 mmol, 1 equiv.) and the corresponding aromatic carbaldehyde(0.122 mmol, 1 equiv.), and the mixture was stirred at room temperature for 2-48 h as determined by TLC. The reaction was quenched with brine (15 mL), and the subsequent mixture was extracted with dichloromethane (10 mL × 3). The combined extracts were dried over anhydrous magnesium sulfate and concentrated in vacuum. The residue was purified over preparative thin layer chromatography, eluting with dichloromethane/methanol (100:5-10, v/v) and/or ethyl acetate/methanol (100:5, v/v), to give the respective product.

*4.3.1 (1E,4E)-1-(1-(sec-Butyl)-1H-imidazol-2-yl)-5-(thiazol-2-yl)penta-1,4-dien-3-one (**25**)*

Yellow oil, 82 % yield. ^{1}H NMR (300 MHz, $CDCl_3$) δ: 7.95 (1H, d, J = 3.3 Hz, thiazole H-4), 7.86 (1H, d, J = 15.9 Hz, vinyl H), 7.65 (1H, d, J = 15.0 Hz, vinyl H), 7.59 (1H, d, J = 15.0 Hz, vinyl H), 7.47 (1H, d, J = 3.3 Hz, thiazole H-5), 7.24 (1H, s, imidazole H-4), 7.23 (1H, d, J = 15.9 Hz, vinyl H), 7.11 (1H, s, imidazole H-5), 4.40 (1H, sextet, J = 7.2 Hz, *sec*-butyl *CH*), 1.88-1.72 (2H, m, *sec*-butyl *CH*$_2$CH$_3$), 1.47 (3H, d, J = 6.6 Hz, *sec*-butyl *CH*$_3$CH), 0.84 (3H, t, J = 7.2 Hz, *sec*-butyl CH$_2$*CH*$_3$). ^{13}C NMR (75 MHz, $CDCl_3$) δ: 188.1, 164.1, 145.2, 143.1, 134.4, 131.3, 130.6, 127.5, 125.8, 121.9, 119.2, 53.6, 31.0, 22.0, 10.7. IR (film) ν_{max}: 3106, 2969, 2930, 1651, 1615, 1589, 1505, 1457, 1419 cm^{-1}. HR-MS (ESI) *m/z*: calcd for $C_{15}H_{18}N_3OS$ $[M+H]^+$: 288.1170; found 288.1166. HPLC purity 95.3% (30 min run of 45-80% CH_3CN in H_2O, with 15 min gradient, 1.0 mL/min).

*4.3.2 (1E,4E)-1-(4-Bromo-1-methyl-1H-pyrazol-3-yl)-5-(1-(sec-butyl)-1H-imidazol-2-yl)penta-1,4-dien-3-one (**26**)*

Yellow oil, 69 % yield. ^{1}H NMR (300 MHz, $CDCl_3$) δ: 7.69 (1H, d, J = 16.2 Hz, vinyl H), 7.68 (1H, d, J = 15.6 Hz, vinyl H), 7.62 (1H, d, J = 15.0 Hz, vinyl H), 7.44 (1H, s, pyrazole H), 7.34 (1H, d, J = 16.2 Hz, vinyl H), 7.28 (1H, s, imidazole H-4), 7.11 (1H, s, imidazole H-5), 4.43 (1H, sextet, J = 7.2

Hz, *sec*-butyl *CH*), 3.95 (3H, s, *N*-CH_3), 1.89-1.73 (2H, m, *sec*-butyl CH_2CH_3), 1.49 (3H, d, *J* = 6.9 Hz, *sec*-butyl CH_3CH), 0.86 (3H, t, *J* = 7.2 Hz, *sec*-butyl CH_2CH_3). ^{13}C NMR (75 MHz, $CDCl_3$) δ: 188.8, 145.3, 143.3, 132.3, 132.1, 131.1, 128.1, 126.8, 126.3, 118.8, 96.2, 53.5, 40.2, 31.0, 22.0, 10.7. IR (film) ν_{max}: 3116, 2971, 2933, 1669, 1623, 1507, 1489, 1457, 1418 cm^{-1}. HR-MS (ESI) *m/z*: calcd for $C_{16}H_{20}BrN_4O$ $[M+H]^+$: 363.0820, 365.0800; found 363.0817, 365.0796. HPLC purity 95.8% (30 min run of 45-80% CH_3CN in H_2O, with 15 min gradient, 1.0 mL/min).

*4.3.3 (1E,4E)-1-(1-(sec-Butyl)-1H-imidazol-2-yl)-5-(5-methylisoxazol-3-yl)penta-1,4-dien-3-one (**27**)*

Yellow oil, 49 % yield. ^{1}H NMR (300 MHz, $CDCl_3$) δ: 7.69 (1H, d, *J* = 16.5 Hz, vinyl H), 7.65 (1H, d, *J* = 16.2 Hz, vinyl H), 7.60 (1H, d, *J* = 16.2 Hz, vinyl H), 7.25 (1H, s, imidazole H-4), 7.12 (1H, s, imidazole H-5), 6.93 (1H, d, *J* = 16.5 Hz, vinyl H), 6.23 (1H, s, isoxazole H-4), 4.41 (1H, sextet, *J* = 6.9 Hz, *sec*-butyl *CH*), 2.47 (3H, s, isoxazole 5-CH_3), 1.87-1.83 (2H, m, *sec*-butyl CH_2CH_3), 1.48 (3H, d, *J* = 6.6Hz, *sec*-butyl CH_3CH), 0.85 (3H, t, *J* = 7.2 Hz, *sec*-butyl CH_2CH_3). ^{13}C NMR (75 MHz, $CDCl_3$) δ: 188.2, 170.5, 160.4, 143.1, 133.1, 131.4, 130.7, 127.8, 125.1, 119.2, 99.7, 53.7, 31.1, 22.0, 12.5, 10.7. IR (film) ν_{max}: 3128, 2970, 2931, 1657, 1630, 1599, 1458, 1268 cm^{-1}. HR-MS (ESI) *m/z*: calcd for $C_{16}H_{20}N_3O_2$ $[M+H]^+$: 286.1556; found 286.1550. HPLC purity 98.7% (30 min run of 45-80% CH_3CN in H_2O, with 15 min gradient, 1.0 mL/min).

*4.3.4 (1E,4E)-1-(1-(sec-Butyl)-1H-imidazol-2-yl)-5-(2-methyl-4-(trifluoromethyl)thiazol-5-yl)penta-1,4-dien-3-one (**28**)*

Yellow solid, mp 79-80 ^{o}C, 79 % yield. ^{1}H NMR (300 MHz, $CDCl_3$) δ: 7.96 (1 H, d, *J* = 15.6 Hz, vinyl H), 7.63 (1H, d, *J* = 17.4 Hz, vinyl H), 7.58 (1H, d, *J* = 17.4 Hz, vinyl H), 7.27 (1H, s, imidazole H-4), 7.12 (1H, d, *J* = 0.6 Hz, imidazole H-5), 6.72 (1H, d, *J* =15.6 Hz, vinyl H), 4.40 (1H, sextet, *J* = 6.9 Hz, *sec*-butyl *CH*), 2.75 (3H, s, thiazole 2-CH_3), 1.87-1.75 (2H, m, *sec*-butyl CH_2CH_3), 1.48 (3H, d, *J* = 6.6 Hz, *sec*-butyl CH_3CH), 0.84 (3H, t, *J* = 7.2 Hz, *sec*-butyl CH_2CH_3). ^{13}C NMR (75 MHz, $CDCl_3$) δ: 187.1, 167.7, 143.5 (J_{CF} = 35 Hz), 142.7, 136.5, 132.3, 130.4, 129.7, 126.8, 126.7, 120.8 (J_{CF} = 270.8 Hz), 119.3, 54.0, 31.0, 22.0, 19.8, 10.7. IR (film) ν_{max}: 3071, 1640, 1603, 1575, 1493, 1387 cm^{-1}. HR-MS (ESI) *m/z*: calcd for $C_{17}H_{19}N_3OF_3S$ $[M+H]^+$: 370.1201; found 370.1198. HPLC purity 96.0% (30 min run of 45-80% CH_3CN in H_2O, with 15 min gradient, 1.0 mL/min).

*4.3.5 (1E,4E)-1-(1-(sec-Butyl)-1H-imidazol-2-yl)-5-(3-methylisoxazol-4-yl)penta-1,4-dien-3-one (**29**)*

Yellow oil, 51 % yield. ^{1}H NMR (300 MHz, $CDCl_3$) δ: 7.71 (1H, d, *J* = 15.0 Hz, vinyl H), 7.59 (1H, d, *J* = 15.0 Hz, vinyl H), 7.57 (1H, d, *J* = 16.2 Hz, vinyl H), 7.28 (1H, s, imidazole H-4), 7.12 (1H, s, imidazole H-5), 7.07 (1H, d, *J* =16.2 Hz, vinyl H), 6.38 (1H, s, isoxazole H-5), 4.41 (1H, sextet, *J* = 7.2

Hz, *sec*-butyl *CH*), 2.33 (3H, s, isoxazole 3-CH_3), 1.87-1.74 (2H, m, *sec*-butyl CH_2CH_3), 1.48 (3H, d, *J* = 6.6 Hz, *sec*-butyl CH_3CH), 0.84 (3H, t, *J* = 7.5 Hz, *sec*-butyl CH_2CH_3). ^{13}C NMR (75 MHz, $CDCl_3$) *δ*: 187.8, 165.9, 160.6, 142.8, 130.7, 130.5, 126.8, 126.6, 126.4, 119.2, 107.9, 53.9, 31.0, 22.0, 11.5, 10.7. IR (film) ν_{max}: 2925, 1647, 1623, 1616, 1577, 1558, 1521, 1507 cm^{-1}. HR-MS (ESI) *m/z*: calcd for $C_{16}H_{20}N_3O_2$ $[M+H]^+$: 286.1555; found 286.1552. HPLC purity 95.8% (30 min run of 45-80% CH_3CN in H_2O, with 15 min gradient, 1.0 mL/min).

*4.3.6 (1E,4E)-1-(1-(sec-Butyl)-1H-imidazol-2-yl)-5-(3,4,5-trimethoxyphenyl)penta-1,4-dien-3-one (**30**)*

Yellow oil, 37 % yield. ^{1}H NMR (300 MHz, $CDCl_3$) *δ*: 8.19 (1H, d, *J* = 15.3 Hz, vinyl H), 7.94 (1H, d, *J* = 16.2 Hz, vinyl H), 7.55 (1H, d, *J* = 15.0 Hz, vinyl H), 7.35 (1H, s, imidazole H-4), 7.15 (1H, s, imidazole H-5), 6.90 (2H, s, phenyl H-2, H-6), 6.86 (1H, d, *J* = 16.2 Hz, vinyl H), 4.52-4.41 (1H, m, *sec*-butyl *CH*), 3.92 (6H, s, 2 × OCH_3), 3.90 (3H, s, OCH_3), 1.93-1.76 (2H, m, *sec*-butyl CH_2CH_3), 1.52 (3H, d, *J* = 6.6Hz, *sec*-butyl CH_3CH), 0.87 (3H, t, *J* = 7.5 Hz, *sec*-butyl CH_2CH_3). ^{13}C NMR (75 MHz, $CDCl_3$) *δ*: 188.5, 153.6, 145.7, 142.7, 140.8, 130.3, 128.9, 128.1, 126.7, 123.5, 118.8, 106.0, 61.2, 56.4, 54.5, 30.8, 21.8, 10.7. IR (film) ν_{max}: 3071, 2927, 1647, 1616, 1581, 1504, 1456, 1419 cm^{-1}. HR-MS (ESI) *m/z*: calcd for $C_{21}H_{26}N_2O_4$ $[M+H]^+$: 371.1971; found 371.1973. HPLC purity 95.3% (30 min run of 45-80% CH_3CN in H_2O, with 15 min gradient, 1.0 mL/min).

*4.3.7 (1E,4E)-1-(1-(sec-Butyl)-1H-imidazol-2-yl)-5-(3,4-dimethoxyphenyl)penta-1,4-dien-3-one (**31**)*

Yellow oil, 19 % yield. ^{1}H NMR (300 MHz, $CDCl_3$) *δ*: 8.14 (1H, d, *J* = 15.0 Hz, vinyl H), 7.95 (1H, d, *J* = 16.2 Hz, vinyl H), 7.56 (1H, d, *J* = 15.0 Hz, vinyl H), 7.34 (1H, s, imidazole H-4), 7.26 (1H, dd, *J* =7.2, 1.8 Hz, phenyl H-6), 7.18 (1H, d, *J* = 1.8 Hz, phenyl H-2), 7.14 (1H, s, imidazole H-5), 6.91 (1H, d, *J* = 8.1 Hz, phenyl H-5), 6.85 (1H, d, *J* = 16.2 Hz, vinyl H), 4.46 (1H, sextet, *J* = 6.9 Hz, *sec*-butyl *CH*), 3.95 (3H, s, OCH_3), 3.94 (3H, s, OCH_3), 1.90-1.78 (2H, m, *sec*-butyl CH_2CH_3), 1.51 (3H, d, *J* = 6.6 Hz, *sec*-butyl CH_3CH), 0.87 (3H, t, *J* = 7.2 Hz, *sec*-butyl CH_2CH_3). ^{13}C NMR (75 MHz, $CDCl_3$) *δ*: 188.5, 151.9, 149.5, 145.6, 142.9, 129.2, 128.8, 127.8, 125.5, 124.0, 123.9, 118.6, 111.3, 110.2, 56.2, 56.1, 54.4, 30.9, 21.9, 10.7. IR (film) ν_{max}: 2966, 2934, 1645, 1615, 1582, 1508, 1458, 1421 cm^{-1}. HR-MS (ESI) *m/z*: calcd for $C_{20}H_{25}N_2O_3$ $[M+H]^+$: 341.1865; found 341.1860. HPLC purity 97.6% (30 min run of 45-80% CH_3CN in H_2O, with 15 min gradient, 1.0 mL/min).

*4.3.8 (1E,4E)-1-(1-(sec-Butyl)-1H-imidazol-2-yl)-5-(6-methylpyridin-2-yl)penta-1,4-dien-3-one (**32**)*

Yellow oil, 72 % yield. ^{1}H NMR (300 MHz, $CDCl_3$) *δ*: 7.87 (1H, d, *J* = 15.3 Hz, vinyl H), 7.80 (1H, d, *J* = 15.9 Hz, vinyl H), 7.60 (1H, t, *J* = 7.8 Hz, pyridine 4-H), 7.59 (1H, d, *J* = 15.0 Hz, vinyl H),

7.44 (1H, d, *J* = 15.9 Hz, vinyl H), 7.30 (1H, d, *J* = 7.8 Hz, pyridine 3-H), 7.27 (1H, s, imidazole H), 7.13 (1H, d, *J* = 7.8 Hz, pyridine 5-H), 7.10 (1H, s, imidazole H), 4.41 (1H, sextet, J = 7.2 Hz, *sec*-butyl *CH*), 2.58 (3H, s, pyridine CH_3), 1.86-1.72 (2H, m, *sec*-butyl CH_2CH_3), 1.47 (3H, d, *J* = 6.9 Hz, *sec*-butyl CH_3CH), 0.84 (3H, t, *J* = 7.5 Hz, *sec*-butyl CH_2CH_3). ^{13}C NMR (75 MHz, $CDCl_3$) δ: 189.1, 159.3, 152.6, 143.2, 143.0, 137.1, 130.2, 130.0, 127.3, 125.8, 124.4, 122.4, 118.8, 53.9, 30.9, 24.8, 21.9, 10.7. IR (film) ν_{max}: 2970, 2932, 1653, 1623, 1616, 1590, 1457 cm^{-1}. HR-MS (ESI) *m/z*: calcd for $C_{18}H_{22}N_3O$ $[M+H]^+$: 296.1763; found 296.1758. HPLC purity 97.7% (30 min run of 45-80% CH_3CN in H_2O, with 15 min gradient, 1.0 mL/min).

*4.3.9 (1E,4E)-1-(Pyridin-2-yl)-5-(thiazol-2-yl)penta-1,4-dien-3-one (**33**)*

Yellow solid, mp 78-79 ^{o}C, 84 % yield. ^{1}H NMR (300 MHz, $CDCl_3$) δ: 8.70 (1H, d, *J* = 3.9 Hz, pyridine H-6), 7.98 (1H, d, *J* = 3.0 Hz, thiazole H-4), 7.89 (1H, d, *J* = 15.9 Hz, vinyl H), 7.80-7.73 (2H, overlapped, vinyl H; pyridine H-4), 7.61 (1H, d, *J* = 15.6 Hz, vinyl H), 7.51 (1H, d, *J* = 7.2 Hz, pyridine H-3), 7.49 (1H, d, *J* = 2.7 Hz, thiazole H-5), 7.39 (1H, d, *J* = 15.9 Hz, vinyl H), 7.32 (1H, dd, *J* = 8.4, 5.7 Hz, pyridine H-5). ^{13}C NMR (75 MHz, $CDCl_3$) δ: 188.8, 164.2, 153.1, 150.4, 145.2, 142.5, 137.2, 134.7, 129.4, 129.5, 125.3, 124.8, 121.8. IR (film) ν_{max}: 3078, 1655, 1622, 1597, 1582, 1467, 1431, 1329 cm^{-1}. HR-MS (ESI) *m/z*: calcd for $C_{13}H_{11}N_2OS$ $[M+H]^+$: 243.0592; found 243.0587. HPLC purity 98.5% (30 min run of 45-80% CH_3CN in H_2O, with 15 min gradient, 1.0 mL/min).

*4.3.10 (1E,4E)-1-(1-(sec-Butyl)-1H-imidazol-2-yl)-5-(pyridin-2-yl)penta-1,4-dien-3-one (**34**)*

Yellow oil, 77 % yield. ^{1}H NMR (300 MHz, $CDCl_3$) δ: 8.69 (1H, d, *J* = 4.5 Hz, pyridine H-6), 7.80 (1H, d, *J* = 15.6 Hz, vinyl H), 7.75–7.72 (2H, overlapped, vinyl H; pyridine H-4), 7.63 (1H, d, *J* = 15.0 Hz, vinyl H), 7.50 (1H, d, *J* = 7.8 Hz, pyridine H-3), 7.47 (1H, d, *J* = 15.6 Hz, vinyl H), 7.31–7.27 (1H, m, pyridine H-5), 7.27 (1H, s, imidazole H-4), 7.11 (1H, d, *J* = 0.9 Hz, imidazole H-5), 4.43 (1H, sextet, *J* = 6.9 Hz, *sec*-butyl *CH*), 1.90–1.74 (2H, m, *sec*-butyl CH_2CH_3), 1.49 (3H, d, *J* = 6.6 Hz, *sec*-butyl CH_3CH), 0.86 (3H, t, *J* = 7.2 Hz, *sec*-butyl CH_2CH_3). ^{13}C NMR (75 MHz, $CDCl_3$) δ: 189.1, 153.3, 150.4, 143.2, 142.3, 137.0, 131.0, 130.2, 127.0, 126.3, 125.1, 124.5, 118.9, 53.6, 31.0, 22.0, 10.7. IR (film) ν_{max}: 3105, 2970, 2932, 1651, 1622, 1585, 1503, 1458, 1431 cm^{-1}. HR-MS (ESI) *m/z*: calcd for $C_{17}H_{20}N_3O$ $[M+H]^+$: 282.1606; found 282.1601. HPLC purity 96.0% (30 min run of 45-80% CH_3CN in H_2O, with 15 min gradient, 1.0 mL/min).

*4.3.11 (1E,4E)-1-(4-Bromo-1-methyl-1H-pyrazol-3-yl)-5-(pyridin-2-yl)penta-1,4-dien-3-one (**35**)*

Yellow solid, mp 81-82 ^{o}C, 71 % yield. ^{1}H NMR (300 MHz, $CDCl_3$) δ: 8.67 (1H, d, *J* = 4.2 Hz, pyridine H-6), 7.76 – 7.74 (1H, dt, *J* = 8.1, 1.8 Hz, pyridine H-4), 7.68 (1H, s, pyrazole H-5), 7.67 (d, *J*

= 16.2 Hz, vinyl H), 7.56 (1H, d, *J* = 15.9 Hz, vinyl H), 7.50-7.42 (2H, overlapped, vinyl H; pyridine H-3), 7.45 (1H, d, *J* = 16.2 Hz, vinyl H), 7.30–7.26 (1H, m, pyridine H-5), 3.93 (3H, s, pyrazole 1-CH_3). ^{13}C NMR (75 MHz, $CDCl_3$) δ: 189.4, 153.4, 150.2, 145.3, 141.7, 137.1, 132.5, 132.1, 129.1, 126.6, 125.0, 124.5, 96.1, 40.2. IR (film) ν_{max}: 3123, 1654, 1628, 1599, 1507, 1466, 1323, 1309 cm^{-1}. HR-MS (ESI) *m/z*: calcd for $C_{14}H_{13}N_3OBr$ $[M+H]^+$: 318.0242, 320.0222; found 318.0239, 320.0218. HPLC purity 96.4% (30 min run of 45-80% CH_3CN in H_2O, with 15 min gradient, 1.0 mL/min).

*4.3.12 (1E,4E)-1-(5-Methylisoxazol-3-yl)-5-(pyridin-2-yl)penta-1,4-dien-3-one (**36**)*

Yellow solid, mp 77-78 ^{o}C, 89 % yield. ^{1}H NMR (300 MHz, $CDCl_3$) δ: 8.68 (1H, d, *J* = 4.0 Hz, pyridine H-6), 7.78– 7.74 (1H, m, pyridine H-4), 7.72 (1H, d, *J* = 16.2 Hz, vinyl H), 7.69 (1H, d, *J* = 16.2 Hz, vinyl H), 7.62 (1H, d, *J* = 15.6 Hz, vinyl H), 7.49 (1H, d, *J* = 7.8 Hz, pyridine H-3), 7.33–7.29 (1H, m, pyridine H-5), 7.04 (1H, d, *J* = 16.2 Hz, vinyl H), 6.24 (1H, s, isoxazole H-3), 2.47 (3H, s, isoxazole 5-CH_3). ^{13}C NMR (75 MHz, $CDCl_3$) δ: 188.9, 170.6, 160.3, 153.0, 150.4, 142.8, 137.1, 132.1, 130.9, 127.6, 125.3, 124.8, 99.7, 12.5. IR (neat) ν_{max}: 3071, 1640, 1603, 1575, 1493, 1387 cm^{-1}. IR (film) ν_{max}: 3051, 2927, 1680, 1660, 1634, 1603, 1463, 1451, 1434 cm^{-1}. HR-MS (ESI) *m/z*: calcd for $C_{14}H_{13}N_2O_2$ $[M+H]^+$: 241.0977; found 241.0972. HPLC purity 97.2% (30 min run of 45-80% CH_3CN in H_2O, with 15 min gradient, 1.0 mL/min).

*4.3.13 (1E,4E)-1-(1-isopropyl-1H-imidazol-2-yl)-5-(2-(pyrrolidin-1-yl)thiazol-5-yl)penta-1,4-dien-3-one (**37**)*

Brown oil, 28% yield. ^{1}H NMR (300 MHz, $CDCl_3$) δ: 7.83 (1H, d, *J* = 15.0 Hz, vinyl H), 7.55 (2H, s, 2 × vinyl H), 7.49 (1H, s, thiazole H-4), 7.19 (1H, s, imidazole H-4), 7.10 (1H, s, imidazole H-5), 6.28 (1H, d, *J* = 15.0 Hz, vinyl H), 4.75-4.60 (1H, m, isopropyl CH), 3.59-3.49 (4H, m, pyrrolidine 2 × CH_2), 2.13-2.04 (4H, m, pyrrolidine 2 × CH_2), 1.53-1.41 (6H, broad peak, isopropyl 2 × CH_3). ^{13}C NMR (75 Hz, $CDCl_3$) δ: 187.8, 169.4, 149.0, 143.1, 135.5, 130.7, 126.8, 125.5, 124.2, 122.9, 118.3, 50.0, 47.7, 25.8, 24.0. IR (neat) ν_{max}: 2923, 2853, 1641, 1607, 1537, 1502, 1458, 1264 cm^{-1}. HR-MS (ESI) *m/z*: calcd for $C_{18}H_{23}N_4OS$ $[M+H]^+$: 343.1593; found 343.1594.

*4.3.14 (1E,4E)-1-(1-isopropyl-1H-imidazol-2-yl)-5-(2-(piperidin-1-yl)thiazol-5-yl)penta-1,4-dien-3-one (**38**)*

Brown-red oil, 63% yield. ^{1}H NMR (300 MHz, $CDCl_3$) δ: 7.83 (1H, d, *J* = 15.3 Hz, vinyl H), 7.57 (1H, d, *J* = 15.3 Hz, vinyl H), 7.52 (1H, d, *J* = 15.3 Hz, vinyl H), 7.45 (1H, s, thiazole H-4), 7.19 (1H, s, imidazole H-4), 7.11 (1H, s, imidazole H-5), 6.27 (1H, d, *J* = 15.3 Hz, vinyl H), 4.68 (1H, hept, *J* = 6.6 Hz, isopropyl CH), 3.58 (4H, br.s, piperidine 2 × CH_2), 1.70 (6H, br.s, piperidine 3 × CH_2), 1.48

(6H, d, J = 6.6 Hz, isopropyl 2 × CH_3). ^{13}C NMR (75 Hz, $CDCl_3$) δ: 187.8, 172.8, 148.6, 143.0, 135.3, 130.7, 126.7, 125.5, 124.2, 123.1, 118.3, 49.9, 47.7, 25.3, 24.2, 24.0. HR-MS (ESI) *m/z*: calcd for $C_{19}H_{25}N_4OS$ $[M+H]^+$: 357.1749; found 357.1747.

*4.3.15 (1E,4E)-1-(1-Isopropyl-1H-imidazol-2-yl)-5-(2-morpholinothiazol-5-yl)penta-1,4-dien-3-one (**39**)*

Brown-red oil, 77% yield. ^{1}H NMR (300 MHz, $CDCl_3$) δ: 7.82 (1H, d, J = 15.3 Hz, vinyl H), 7.59 (1H, d, J = 15.0 Hz, vinyl H), 7.53 (1H, d, J = 15.0 Hz, vinyl H), 7.47 (1H, s, thiazole H-4), 7.20 (1H, s, imidazole H-4), 7.12 (1H, s, imidazole H-5), 6.32 (1H, d, J = 15.3 Hz, vinyl H), 4.69 (1H, hept, J = 6.6 Hz, isopropyl CH), 3.83 (4H, t, J = 4.8 Hz, morpholine 2 × OCH_2), 3.59 (4H, t, J = 4.8 Hz, morpholine 2 × NCH_2), 1.48 (6H, d, J = 6.6 Hz, isopropyl 2 × CH_3). ^{13}C NMR (75 Hz, $CDCl_3$) δ: 187.8, 172.8, 147.8, 142.9, 134.8, 130.8, 126.4, 125.9, 125.2, 124.1, 118.5, 66.2, 48.5, 47.7, 24.0. IR (film) ν_{max}: 2937, 2855, 1640, 1608, 1529, 1504, 1461, 1308, 1267 cm^{-1}. HR-MS (ESI) *m/z*: calcd for $C_{18}H_{23}N_4O_2S$ $[M+H]^+$: 359.1542; found 359.1538. HPLC purity 98.2% (30 min run of 45-80% CH_3CN in H_2O, with 15 min gradient, 1.0 mL/min).

*4.3.16 (1E,4E)-1-(1-Isopropyl-1H-imidazol-2-yl)-5-(4-methyl-2-(pyridine-4-yl)thiazol-5-yl)penta-1,4-dien-3-one (**40**)*

Yellow oil, 55% yield. ^{1}H NMR (300 MHz, $CDCl_3$) δ: 8.73 (2H, d, J = 6.0 Hz, pyridine 2-H & 6-H), 7.92 (1H, d, J = 15.3 Hz, vinyl H), 7.81 (2H, d, J = 6.0 Hz, pyridine H-3 & H-5), 7.64 (2H, s, 2 × vinyl H), 7.25 (1H, s, imidazole H-4), 7.16 (1H, s, imidazole H-5), 6.71 (1H, d, J = 15.6 Hz, vinyl H), 4.77-4.66 (1H, m, isopropyl CH), 2.65 (3H, s, thiazole 4-CH_3), 1.51 (6H, d, J = 6.6 Hz, isopropyl 2 × CH_3). ^{13}C NMR (75MHz, $CDCl_3$) δ: 187.6, 164.7, 158.3, 150.9, 142.6, 139.8, 132.3, 131.4, 131.1, 129.2, 127.5, 127.0, 120.5, 118.9, 47.8, 24.0, 16.1. IR (film) ν_{max}: 2979, 2923, 1647, 1611, 1595, 1578, 1461, 1270 cm^{-1}. HR-MS (ESI) *m/z*: calcd for $C_{20}H_{21}N_4OS$ $[M+H]^+$: 365.1436; found 365.1431. HPLC purity 96.0% (30 min run of 45-80% CH_3CN in H_2O, with 15 min gradient, 1.0 mL/min).

*4.3.17 (1E,4E)-1-(1-Isopropyl-1H-benzo[d]imidazole-2-yl)-5-(1-isopropyl-1H-imidazole-2-yl)penta-1,4-dien-3-one (**41**)*

This compound was prepared in 43% yield as a yellow oil. ^{1}H NMR (300 MHz, $CDCl_3$) δ: 7.84 (1H, d, J = 15.2 Hz, vinyl H), 7.82–7.75 (overlapped, 1H, benzoimidazole H), 7.78 (1H, d, J = 15.2 Hz, vinyl H), 7.68 (1H, d, J = 15.2 Hz, vinyl H), 7.56–7.51 (1H, overlapped, benzoimidazole H), 7.54 (1H, d, J = 15.2 Hz, vinyl H), 7.31–7.26 (2H, m, 2 × benzoimidazole H), 7.24 (1H, s, imidazole H-4), 7.15 (1H, s, imidazole H-5), 4.99 (1H, hept, J = 7.2 Hz, isopropyl CH), 4.70 (1H, hept, J = 6.9 Hz,

isopropyl CH), 1.69 (6H, d, J = 6.9 Hz, isopropyl 2 × CH_3), 1.49 (6H, d, J = 6.6 Hz, isopropyl 2 × CH_3). ^{13}C NMR (75 MHz, $CDCl_3$) δ: 188.0, 147.8, 144.0, 142.4, 134.5, 132.2, 131.3, 127.8, 127.6, 127.1, 123.7, 123.2, 120.7, 119.0, 112.2, 48.2, 47.8, 24.0, 22.0. IR (film) ν_{max}: 2978, 2935, 2878, 1651, 1619, 1589, 1460, 1383, 1266, 1100 cm^{-1}. HR-MS (ESI) *m/z*: calcd for $C_{21}H_{25}N_4O$ $[M+H]^+$: 349.2028; found 349.2027. HPLC purity 99.4% (30 min run of 45-80% CH_3CN in H_2O, with 15 min gradient, 1.0 mL/min).

*4.3.18 (1E,4E)-1-(1-(sec-Butyl)-1H-benzo[d]imidazole-2-yl)-5-(1-(sec-butyl)-1H-imidazole-2-yl)penta-1,4-dien-3-one (**42**)*

This compound was prepared in 49% yield as a yellow oil. ^{1}H NMR (300 MHz, $CDCl_3$) δ: 7.83–7.81 (3H, m, 2 × vinyl H; 1 × benzoimidazole H), 7.69 (1H, d, J = 15.3 Hz, vinyl H), 7.60–7.50 (2H, overlapped, 1× vinyl H; 1 × benzoimidazole H), 7.33–7.25 (3H, m, 2 × benzoimidazole H; imidazole H-4), 7.13 (1H, s, imidazole H-5), 4.75–4.62 (1H, m, *sec*-butyl CH), 4.48–4.38 (1H, m, *sec*-butyl CH), 2.28–2.12 (1H, m, *sec*-butyl CH_2CH_3), 2.05–1.95 (1H, m, *sec*-butyl CH_2CH_3), 1.88–1.75 (2H, m, *sec*-butyl CH_2CH_3), 1.70 (3H, d, J = 7.2 Hz, *sec*-butyl CH_3CH), 1.49 (3H, d, J = 6.6 Hz, *sec*-butyl CH_3CH), 0.86 (3H, t, J = 7.4 Hz, *sec*-butyl CH_2CH_3), 0.80 (3H, t, J = 7.4 Hz, *sec*-butyl CH_2CH_3). ^{13}C NMR (75 MHz, $CDCl_3$) δ: 188.1, 148.5, 143.9, 143.0, 134.6, 132.2, 131.4, 127.9, 127.7, 127.2, 123.7, 123.2, 120.7, 119.2, 112.2, 54.4, 53.6, 31.0, 28.7, 22.1, 20.4, 11.3, 10.7. IR (film) ν_{max}: 2969, 2934, 2877, 1651, 1620, 1457, 1384, 1290, 1178 cm^{-1}. HR-MS (ESI) *m/z*: calcd for $C_{23}H_{29}N_4O$ $[M+H]^+$: 377.2341; found 377.2337. HPLC purity 95.0% (30 min run of 45-80% CH_3CN in H_2O, with 15 min gradient, 1.0 mL/min).

*4.3.19 (1E,4E)-1-(1-Isobutyl-1H-benzo[d]imidazole-2-yl)-5-(1-isobutyl-1H-imidazole-2-yl)penta-1,4-dien-3-one (**43**)*

This compound was prepared in 35% yield as a yellow oil. ^{1}H NMR (300 MHz, $CDCl_3$) δ: 7.81 (1H, d, J = 15.2 Hz, vinyl H), 7.83–7.76 (1H, m, benzoimidazole H), 7.73 (1H, d, J = 15.3 Hz, vinyl H), 7.61 (1H, d, J = 15.3 Hz, vinyl H), 7.49 (1H, d, J = 15.3 Hz, vinyl H), 7.39–7.30 (3H, m, 3 × benzoimidazole H), 7.23 (1H, d, J = 0.9 Hz, imidazole H-4), 7.04 (1H, d, J = 0.9 Hz, imidazole H-5), 4.12 (2H, d, J = 7.5 Hz, isobutyl CH_2), 3.89 (2H, d, J = 7.5 Hz, isobutyl CH_2), 2.30–2.18 (1H, m, isobutyl CH), 2.09– 2.00 (1H, m, isobutyl CH_2, 0.97 (6H, d, J = 6.6 Hz, isobutyl 2 × CH_3), 0.95 (6H, d, J = 6.6 Hz, isobutyl 2 × CH_3). ^{13}C NMR (75 MHz, $CDCl_3$) δ: 187.9, 148.6, 143.4, 136.3, 131.8, 131.0, 127.8, 127.5, 127.2, 124.1, 123.7, 123.5, 120.5, 110.5, 53.8, 51.2, 30.8, 30.1, 20.4, 20.1. IR (film) ν_{max}:

3043, 2962, 2873, 1652, 1622, 1592, 1404, 1091 cm^{-1}. HR-MS (ESI) *m/z*: calcd for $C_{23}H_{29}N_4O$ $[M+H]^+$: 377.2341; found 377.2333. HPLC purity 95.0% (30 min run of 45-80% CH_3CN in H_2O, with 15 min gradient, 1.0 mL/min).

*4.3.20 (1E,4E)-1-(1-Isopentyl-1H-benzo[d]imidazole-2-yl)-5-(1-isopentyl-1H-imidazole-2-yl)penta-1,4-dien-3-one (**44**)*

This compound was prepared in 35% yield as a yellow oil. ^{1}H NMR (300 MHz, $CDCl_3$) δ: 7.81 (1H, d, *J* = 15.3 Hz, vinyl H), 7.81–7.78 (1H, m, benzoimidazole H), 7.75 (1H, d, *J* = 15.3 Hz, vinyl H), 7.64 (1H, d, *J* = 15.0 Hz, vinyl H), 7.50 (1H, d, *J* = 15.0 Hz, vinyl H), 7.38–7.27 (3H, m, 3 × benzoimidazole H), 7.23 (1H, s, imidazole H-4), 7.07 (1H, s, imidazole H-5), 4.31(2H, t, *J* = 7.4 Hz, isopentyl *N*-CH_2), 4.10 (2H, t, *J* = 7.5 Hz, isopentyl *N*-CH_2), 1.71–1.60 (6H, m, 2 × isopentyl *N*-CH_2*CH_2CH*), 1.01 (6H, d, *J* = 5.9 Hz, isopentyl CH*$(CH_3)_2$*), 0.97 (6H, d, *J* = 6.2 Hz, isopentyl CH*$(CH_3)_2$*). ^{13}C NMR (75 MHz, $CDCl_3$) δ: 187.9, 148.1, 143.5, 143.0, 135.9, 131.8, 131.1, 127.7, 127.24, 127.19, 124.2, 123.5, 123.1, 120.6, 110.0, 44.8, 42.4, 40.5, 39.6, 26.1, 25.8, 22.6, 22.5. IR (film) ν_{max}: 2956, 2928, 2870, 1652, 1622, 1447, 1406, 1094 cm^{-1}. HR-MS (ESI) *m/z*: calcd for $C_{25}H_{33}N_4O$ $[M+H]^+$: 405.2654; found 405.2648. HPLC purity 96.1% (30 min run of 45-80% CH_3CN in H_2O, with 15 min gradient, 1.0 mL/min).

*4.3.21 (1E,4E)-1-(1-(Pentan-2-yl)-1H-benzo[d]imidazole-2-yl)-5-(1-(pentan-2-yl)-1H-imidazole-2-yl)penta-1,4-dien-3-one (**45**)*

This compound was prepared in 81% yield as a yellow oil. ^{1}H NMR (300 MHz, $CDCl_3$) δ: 7.84–7.78 (3H, m, 2 × vinyl H; 1 × benzoimidazole), 7.69 (1H, d, *J* = 15.0 Hz, vinyl H), 7.58–7.52 (2H, m, 1× vinyl H; 1× benzoimidazole H), 7.34– 7.28 (3H, m, 2 × benzoimidazole H; imidazole H-4), 7.13 (1H, d, *J* = 0.9 Hz, imidazole H-5), 4.81–4.74 (1H, m, 1-(pentan-2-yl) CH), 4.56–4.49 (1H, m, 1-(pentan-2-yl) CH), 2.23–2.12 (2H, m, 1-(pentan-2-yl) CH*CH_2*CH_2CH_3), 1.97–1.89 (1H, m, 1-(pentan-2-yl) CH*CH_2*CH_2CH_3), 1.77 (2H, q, *J* = 7.6 Hz, 1-(pentan-2-yl) CH*CH_2*CH_2CH_3), 1.70 (3H, d, *J* = 6.9 Hz, 1-(pentan-2-yl) *CH_3*CH), 1.49 (3H, d, *J* = 6.7 Hz, 1-(pentan-2-yl) *CH_3*CH), 1.28 – 1.15 (3H, m, 1-(pentan-2-yl) CH*CH_2*CH_2*CH_2*CH_3), 0.91 (3H, t, *J* = 7.3 Hz, 1-(pentan-2-yl) $CHCH_2CH_2$*CH_3*), 0.87 (3H, t, *J* = 7.2 Hz, 1-(pentan-2-yl) $CHCH_2CH_2$*CH_3*). ^{13}C NMR (75 MHz, $CDCl_3$) δ: 188.1, 148.4, 144.0, 143.0, 134.6, 132.2, 131.5, 127.9, 127.8, 127.2, 123.7, 123.2, 120.8, 119.2, 112.2, 52.7, 52.0, 40.1, 37.8, 22.5, 20.7, 20.1, 19.5, 13.9, 13.8. IR (film) ν_{max}: 2959, 2932, 2873, 1651, 1619, 1455, 1382, 1175 cm^{-1}. HR-MS (ESI) *m/z*: calcd for $C_{25}H_{33}N_4O$ $[M+H]^+$: 405.2654; found 405.2650. HPLC purity 97.9% (30 min run of 45-80% CH_3CN in H_2O, with 15 min gradient, 1.0 mL/min).

*4.3.22 (1E,4E)-1-(1-Propyl-1H-benzo[d]imidazole-2-yl)-5-(1-propyl-1H-imidazole-2-yl)penta-1,4-dien-3-one (**46**)*

This compound was prepared in 38% yield as a yellow oil. ^{1}H NMR (300 MHz, $CDCl_3$) δ: 7.83 (1H, d, J = 15.2 Hz, vinyl H), 7.84 –7.78 (1H, m, benzoimidazole H), 7.74 (1H, d, J = 15.2 Hz, vinyl H), 7.63 (1H, d, J = 15.2 Hz, vinyl H), 7.51 (1H, d, J = 15.2 Hz, vinyl H), 7.42–7.30 (3H, m, 3 × benzoimidazole H), 7.23 (1H, d, J = 0.7 Hz, imidazole H-4), 7.08 (1H, d, J = 1.0 Hz, imidazole H-5), 4.30 (2H, t, J = 7.2 Hz, propyl $N$$CH_2$), 4.08 (2H, t, J = 7.2 Hz, propyl $N$$CH_2$), 1.95–1.79 (4H, m, 2 × CH_2*CH_2*CH_3), 0.982 (3H, t, J = 7.5 Hz, propyl CH_3), 0.977 (3H, t, J = 7.5 Hz, propyl CH_3). ^{13}C NMR (75 MHz, $CDCl_3$) δ: 187.9, 148.3, 143.4, 143.1, 136.0, 131.7, 131.1, 127.7, 127.2, 127.1, 124.1, 123.5, 123.3, 120.5, 110.2, 48.0, 45.4, 24.9, 24.0, 11.5, 11.3. IR (film) ν_{max}: 2966, 2932, 1652, 1624, 1597, 1446, 1408, 1096 cm^{-1}. HR-MS (ESI) *m/z*: calcd for $C_{21}H_{25}N_4O$ $[M+H]^+$: 349.2028; found 349.2023. HPLC purity 95.9% (30 min run of 45-80% CH_3CN in H_2O, with 15 min gradient, 1.0 mL/min).

*4.3.23 (1E,4E)-1-(1-Butyl-1H-benzo[d]imidazole-2-yl)-5-(1-butyl-1H-imidazole-2-yl)penta-1,4-dien-3-one (**47**)*

This compound was prepared in 50% yield as a yellow oil. ^{1}H NMR (300 MHz, $CDCl_3$) δ: 7.83 (1H, d, J = 15.3 Hz, vinyl H), 7.83–7.80 (1H, m, benzoimidazole H), 7.75 (1H, d, J = 15.3 Hz, vinyl H), 7.64 (1H, d, J = 15.3 Hz, vinyl H), 7.51 (1H, d, J = 15.3 Hz, vinyl H), 7.40–7.30 (3H, m, 3 × benzoimidazole H), 7.24 (1H, d, J = 0.7 Hz, imidazole H-4), 7.07 (1H, d, J = 1.0 Hz, imidazole H-5), 4.33 (2H, t, J = 7.2 Hz, butyl $N$$CH_2$), 4.10 (2H, t, J = 7.2 Hz, butyl $N$$CH_2$), 1.87–1.74 (4H, m, 2 × butyl $N$$CH_2$*$CH_2$*), 1.39–1.32 (4H, m, 2 × butyl $N$$CH_2CH_2$*$CH_2$*), 0.97 (3H, t, J = 7.2 Hz, butyl CH_3), 0.96 (3H, t, J = 7.2 Hz, butyl CH_3). ^{13}C NMR (75 MHz, $CDCl_3$) δ: 188.0, 148.3, 143.6, 143.1, 136.1, 131.9, 131.2, 127.8, 127.32, 127.25, 124.2, 123.6, 123.3, 120.6, 110.2, 46.4, 43.8, 33.7, 32.9, 20.4, 20.1, 13.9, 13.8. IR (film) ν_{max}: 2960, 2931, 2874, 1653, 1624, 1446, 1408, 1264 cm^{-1}. HR-MS (ESI) *m/z*: calcd for $C_{23}H_{29}N_4O$ $[M+H]^+$: 377.2341; found 377.2336. HPLC purity 97.3% (30 min run of 45-80% CH_3CN in H_2O, with 15 min gradient, 1.0 mL/min).

*4.3.24 (1E,4E)-1-(1-Methyl-1H-benzo[d]imidazol-2-yl)-5-(2-methyl-4-(trifluoromethyl)thiazol-5-yl)penta-1,4-dien-3-one (**48**)*

Yellow solid, mp 134-135 ^{o}C, 34 % yield. ^{1}H NMR (300 MHz, $CDCl_3$) δ: 7.98 (1H, d, J = 15.6 Hz, vinyl H), 7.77 (1H, d, J = 8.7 Hz, benzoimidazole H), 7.76 (2H, s, 2 × vinyl H), 7.35-7.31 (3H, overlapped, 3 × benzoimidazole H), 6.73 (1H, d, J = 15.6 Hz, vinyl H), 3.90 (3H, s, benzoimidazole

CH_3), 2.75 (3H, s, thiazole CH_3). ^{13}C NMR (75 MHz, $CDCl_3$) δ: 186.7, 168.1, 148.2, 143.7 (J_{CF} = 35.2 Hz), 143.2, 136.5, 136.3, 131.8, 130.3, 130.1, 127.8, 124.5, 123.8, 120.8 (J_{CF} = 270.8 Hz), 120.4, 110.0, 30.2, 19.8. IR (film) ν_{max}: 2920, 1669, 1623, 1588, 1458, 1367, 1334, 1169, 1111 cm^{-1}. HR-MS (ESI) *m/z*: calcd for $C_{18}H_{15}N_3OSF_3$ $[M+H]^+$: 378.0888; found 378.0878. HPLC purity 97.0% (30 min run of 45-80% CH_3CN in H_2O, with 15 min gradient, 1.0 mL/min).

*4.3.25 (1E,4E)-1-(1-Ethyl-1H-benzo[d]imidazol-2-yl)-5-(2-methyl-4-(trifluoromethyl)thiazol-5-yl)penta-1,4-dien-3-one (**49**)*

Yellow solid, mp 133-134^oC, 89 % yield. ^1H NMR (300 MHz, $CDCl_3$) δ: 8.02 (1H, d, *J* = 15.9 Hz, vinyl H), 7.93-7.82 (2H, m, 1 × vinyl H; 1 × benzoimidazole H), 7.76 (1H, d, *J* = 15.0 Hz, vinyl H), 7.41-7.34 (3H, overlapped, 3 × benzoimidazole H), 6.78 (1H, d, *J* = 15.6 Hz, vinyl H), 4.40 (2H, q, *J* = 7.5 Hz, ethyl CH_2), 2.77 (3H, s, thiazole CH_3), 1.49 (3H, t, *J* = 7.5 Hz, ethyl CH_3). ^{13}C NMR (75 MHz, $CDCl_3$) δ: 186.7, 168.1, 147.5, 143.7 (q, J_{CF} = 35.3 Hz), 143.4, 136.3, 135.5, 131.9, 130.3, 130.2, 127.7, 124.4, 123.8, 120.8 (q, J_{CF} = 270.8 Hz), 120.5, 110.0, 38.8, 19.8, 16.0. IR (film) ν_{max}: 2980, 1653, 1621, 1540, 1409, 1363 cm^{-1}. HR-MS (ESI) *m/z*: calcd for $C_{19}H_{17}N_3OSF_3$ $[M+H]^+$: 392.1044; found 392.1037. HPLC purity 97.1% (30 min run of 45-80% CH_3CN in H_2O, with 15 min gradient, 1.0 mL/min).

*4.3.26 (1E,4E)-1-(2-Methyl-4-(trifluoromethyl)thiazol-5-yl)-5-(1-propyl-1H-benzo[d]imidazol-2-yl)penta-1,4-dien-3-one (**50**)*

Yellow solid, mp 145-146 ^oC, 59 % yield. ^1H NMR (300 MHz, $CDCl_3$) δ: 7.99 (1H, d, *J* = 15.6 Hz, vinyl H), 7.81 (1H, d, *J* = 15.0 Hz, vinyl H), 7.79 (1H, t, *J* = 4.2 Hz, benzoimidazole H), 7.73 (1H, d, *J* = 15.0 Hz, vinyl H), 7.40-7.28 (3H, overlapped, 3 × benzoimidazole H), 6.76 (1H, d, *J* = 15.6 Hz, vinyl H), 4.27 (2H, t, *J* = 7.2 Hz, propyl *N*-CH_2), 2.72 (3H, s, thiazole CH_3), 1.93-1.83 (2H, m, propyl *N*-CH_2CH_2), 0.95 (3H, t, *J* = 7.2 Hz, propyl CH_3). ^{13}C NMR (75 MHz, $CDCl_3$) δ: 186.7, 168.1, 147.9, 143.7 (q, J_{CF} = 36 Hz), 143.3, 136.3, 136.0, 131.9, 130.3, 130.1, 127.9, 124.4, 123.7, 120.8 (q, J_{CF} = 270.8 Hz), 120.5, 110.3, 45.5, 24.1, 19.8, 11.5. IR (film) ν_{max}: 2968, 1699, 1622, 1507, 1472, 1363 cm^{-1}. HR-MS (ESI) *m/z*: calcd for $C_{20}H_{19}N_3OSF_3$ $[M+H]^+$: 406.1201; found 406.1194. HPLC purity 96.2% (30 min run of 45-80% CH_3CN in H_2O, with 15 min gradient, 1.0 mL/min).

*4.3.27 (1E,4E)-1-(1-Isopropyl-1H-benzo[d]imidazol-2-yl)-5-(2-methyl-4-(trifluoromethyl)thiazol-5-yl)penta-1,4-dien-3-one (**51**)*

Yellow syrup, 54 % yield. ^1H NMR (300 MHz, $CDCl_3$) δ: 8.00 (1H, d, *J* = 15.9 Hz, vinyl H), 7.87-7.7.75 (3H, overlapped, 2 × vinyl H; 1 × benzoimidazole H), 7.57-7.54 (1H, m, benzoimidazole H),

7.31-7.26 (2H, overlapped, 2 × benzoimidazole H), 6.76 (1H, d, *J* = 15.6 Hz, vinyl H), 4.99-4.92 (1H, m, isopropyl CH), 2.74 (3H, s, thiazole CH_3), 1.69 (6H, d, *J* = 7.2 Hz, isopropyl 2 × CH_3). IR (film) ν_{max}: 2980, 1653, 1618, 1488, 1386, 1165 cm^{-1}. HR-MS (ESI) *m/z*: calcd for $C_{20}H_{19}N_3OSF_3$ $[M+H]^+$: 406.1201; found 406.1197. HPLC purity 95.0% (30 min run of 45-80% CH_3CN in H_2O, with 15 min gradient, 1.0 mL/min).

*4.3.28 (1E,4E)-1-(Pyridin-2-yl)-5-(3,4,5-trimethoxyphenyl)penta-1,4-dien-3-one (**52**)*

Yellow oil, 42 % yield. ^1H NMR (300 MHz, $CDCl_3$) δ: 8.70 (1H, d, *J* = 4.8 Hz, pyridine H-6), 7.80-7.71 (4H, overlapped, 3 × vinyl H; pyridine H-4), 7.51 (1H, d, *J* = 7.7 Hz, pyridine H-3), 7.32 (1H, dd, *J* = 7.1, 5.2 Hz, pyridine H-5), 6.99 (1H, d, *J* = 16.0 Hz, vinyl H), 6.86, (2H, s, phenyl H-2, H-6), 3.93 (6H, s, phenyl 3-OCH_3, 5-OCH_3), 3.91 (3H, s, phenyl 4-OCH_3). ^{13}C NMR (75 MHz, $CDCl_3$) δ: 189.2, 153.7, 153.3, 150.1, 144.3, 141.2, 140.6, 137.4, 130.3, 128.5, 125.6, 125.4, 124.6, 105.8, 61.2, 56.3. IR (film) ν_{max}: 3071, 2939, 2839, 1653, 1623, 1579, 1503, 1464, 1431, 1419, 1320 cm^{-1}. HR-MS (ESI) *m/z*: calcd for $C_{19}H_{20}NO_4$ $[M+H]^+$: 326.1392; found 326.1387. HPLC purity 98.4% (30 min run of 45-80% CH_3CN in H_2O, with 15 min gradient, 1.0 mL/min).

*4.3.29 (1E,4E)-1-(6-Methylpyridin-2-yl)-5-(pyridin-2-yl)penta-1,4-dien-3-one (**53**)*

Brown solid, mp 43-44 ^oC, 80 % yield. ^1H NMR (300 MHz, $CDCl_3$) δ: 8.68 (1H, d, *J* = 4.5 Hz, pyridine H-6), 7.79-7.72 (3H, overlapped, 2 × vinyl H, pyridine H-4), 7.67-7.58 (3H, overlapped, 2 × vinyl H, methylpyridine H-4), 7.51 (1H, d, *J* = 7.8 Hz, pyridine H-3), 7.34-7.27 (2H, overlapped, pyridine H-5, methylpyridine H-3), 7.16 (1H, d, *J* = 7.7 Hz, methylpyridine H-5), 2.62 (3H, s, methylpyridine CH_3). ^{13}C NMR (75 MHz, $CDCl_3$) δ: 189.8, 159.2, 153.4, 152.6, 150.3, 142.5, 142.2, 137.2, 137.0, 129.0, 128.8, 125.0, 124.5, 124.5, 122.2, 24.5. IR (film) ν_{max}: 3054, 1655, 1628, 1603, 1582, 1451, 1331 cm^{-1}. HR-MS (ESI) *m/z*: calcd for $C_{16}H_{15}N_2O$ $[M+H]^+$: 251.1184; found 251.1179. HPLC purity 95.2% (30 min run of 45-80% CH_3CN in H_2O, with 15 min gradient, 1.0 mL/min).

*4.3.30 (1E,4E)-1-(3,4-Dimethoxyphenyl)-5-(pyridin-2-yl)penta-1,4-dien-3-one (**54**)*

Yellow oil, 21 % yield. ^1H NMR (300 MHz, $CDCl_3$) δ: 8.71 (1H, d, *J* = 4.7 Hz, pyridine H-6), 7.82–7.72 (4H, overlapped, 3 × vinyl H, pyridine H-4), 7.52 (1H, d, *J* = 7.8 Hz, pyridine H-3), 7.34 (1H, dd, *J* = 7.2, 5.1 Hz, pyridine H-5), 7.23 (1H, dd, *J* = 8.3, 1.8 Hz, phenyl H-6), 7.16 (1H, d, *J* = 1.8 Hz, phenyl H-2), 6.97 (1H, d, *J* = 16.2 Hz, vinyl H), 6.91 (1H, d, *J* = 8.4 Hz, phenyl H-5), 3.95 (3H, s, OCH_3), 3.94 (3H, s, OCH_3). IR (film) ν_{max}: 2925, 1651, 1623, 1588, 1265 cm^{-1}. HR-MS (ESI) *m/z*: calcd for $C_{18}H_{18}NO_3$ $[M+H]^+$: 296.1287; found 296.1281. HPLC purity 96.3% (30 min run of 45-80% CH_3CN in H_2O, with 15 min gradient, 1.0 mL/min).

*4.3.31 (1E,4E)-1-(1-Methyl-1H-benzo[d]imidazol-2-yl)-5-(pyridin-2-yl)penta-1,4-dien-3-one (**55**)*

Yellow solid, mp 65-66^{o}C, 52 % yield. ^{1}H NMR (300 MHz, $CDCl_3$) δ: 8.70 (1H, d, J = 4.2 Hz, pyridine H-6), 8.02 (1H, d, J = 15.0 Hz, vinyl H), 7.85 (1H, d, J = 15.9 Hz, vinyl H), 7.81 (1H, d, J = 15.3 Hz, vinyl H), 7.85-7.75 (2H, overlapped, pyridine H-4; 1 × benzoimidazole H), 7.53 (1H d, J = 15.0 Hz, vinyl H), 7.51 (1H, d, J = 8.1 Hz, pyridine H-3), 7.39-7.29 (4H, overlapped, pyridine H-5; 3 × benzoimidazole H), 3.95 (3H, s, CH_3). ^{13}C NMR (75 MHz, $CDCl_3$) δ: 188.7, 153.2, 150.5, 148.6, 143.2, 137.1, 136.5, 130.7, 130.0, 127.0, 125.3, 124.8, 124.4, 123.8, 120.4, 110.0, 30.3. IR (film) ν_{max}: 3053, 2928, 1655, 1615, 1471, 1330 cm^{-1}. HR-MS (ESI) *m/z*: calcd for $C_{18}H_{16}N_3O$ $[M+H]^+$: 290.1293; found 290.1287. HPLC purity 98.5% (30 min run of 45-80% CH_3CN in H_2O, with 15 min gradient, 1.0 mL/min).

*4.3.32 (1E,4E)-1-(1-Ethyl-1H-benzo[d]imidazol-2-yl)-5-(pyridin-2-yl)penta-1,4-dien-3-one (**56**)*

Yellow oil, 34 % yield. ^{1}H NMR (300 MHz, $CDCl_3$) δ: 8.69 (1H, d, J = 3.9 Hz, pyridine H-6), 7.99 (1H, d, J = 15.3 Hz, vinyl H), 7.85-7.77 (4H, overlapped, 2 × vinyl H; pyridine H-4; 1 × benzoimidazole H), 7.51 (1H, d, J = 15.9 Hz, vinyl H), 7.50 (1H, d, J = 8.1 H, pyridine H-3), 7.42-7.26 (4H, overlapped, pyridine H-5; 3 × benzoimidazole H), 4.38 (2H, q, J = 7.5 Hz, ethyl CH_2), 1.48 (3H, t, J = 7.2 Hz, ethyl CH_3). ^{13}C NMR (75 MHz, $CDCl_3$) δ: 188.6, 153.1, 150.4, 147.8, 143.4, 143.0, 136.9, 135.5, 130.4, 129.9, 127.1, 125.1, 124.6, 124.1, 123.5, 120.4, 109.9, 38.7, 16.0. IR (film) ν_{max}: 3058, 2976, 1655, 1627, 1601, 1564, 1470, 1326 cm^{-1}. HR-MS (ESI) *m/z*: calcd for $C_{19}H_{18}N_3O$ $[M+H]^+$: 304.1450; found 304.1444. HPLC purity 99.0% (30 min run of 45-80% CH_3CN in H_2O, with 15 min gradient, 1.0 mL/min).

*4.3.33 (1E,4E)-1-(1-Propyl-1H-benzo[d]imidazol-2-yl)-5-(pyridin-2-yl)penta-1,4-dien-3-one (**57**)*

Brown syrup, 39 % yield. ^{1}H NMR (300 MHz, $CDCl_3$) δ: 8.69 (1H, d, J = 4.5 Hz, pyridine H-6), 8.02 (1H, d, J = 15.3 Hz, vinyl H), 7.86-7.73 (4H, overlapped, 2 × vinyl H; pyridine H-4; 1 × benzoimidazole H), 7.51 (1H, d, J = 9.9 Hz, pyridine H-3), 7.50 (1H, d, J = 15.6 Hz, vinyl H), 7.42-7.28 (4H, overlapped, pyridine H-5; 3 × benzoimidazole H), 4.30 (2H, t, J = 7.2 Hz, propyl *N*-CH_2), 1.89 (2H, sextet, J = 7.2 Hz, propyl *N*-CH_2CH_2), 0.98 (3H, t, J = 7.2 Hz, propyl CH_3). ^{13}C NMR (75 MHz, $CDCl_3$) δ: 188.7, 153.2, 150.5, 148.3, 143.4, 143.0, 137.0, 136.0, 130.4, 130.1, 127.3, 125.1, 124.7, 124.1, 123.5, 120.5, 110.2, 45.4, 24.1, 11.5. IR (film) ν_{max}: 3069, 2964, 2930, 1655, 1627, 1599, 1465, 1407, 1326 cm^{-1}. HR-MS (ESI) *m/z*: calcd for $C_{20}H_{20}N_3O$ $[M+H]^+$: 318.1606; found 318.1601. HPLC purity 96.3% (30 min run of 45-80% CH_3CN in H_2O, with 15 min gradient, 1.0 mL/min).

*4.3.34 (1E,4E)-1-(1-Isopropyl-1H-benzo[d]imidazol-2-yl)-5-(pyridin-2-yl)penta-1,4-dien-3-one (**58**)*

Brown oil, 79 % yield. ^{1}H NMR (300 MHz, $CDCl_3$) δ: 8.67 (1H, d, J = 4.5 Hz, pyridine H-6), 7.98 (1H, d, J = 15 Hz, vinyl H), 7.85 (1H, d, J = 15.0 Hz, vinyl H), 7.823 (1H, t, J = 5.7 Hz, benzoimidazole H), 7.817 (1H, d, J = 15.3 Hz, vinyl H), 7.71 (1H, t, J = 7.5 Hz, pyridine H-4), 7.58-7.47 (3H, overlapped, 1 × vinyl H; pyridine H-3; 1 × benzoimidazole H), 7.30-7.26 (3H, overlapped, 2 × benzoimidazole H; pyridine H-5), 4.99 (1H, septet, J = 6.9 Hz, isopropyl CH), 1.69 (6H, d, J = 6.9 Hz, isopropyl 2 × CH_3). ^{13}C NMR (75 MHz, $CDCl_3$) δ: 188.7, 153.1, 150.4, 147.7, 143.8, 142.9, 136.9, 134.4, 130.7, 129.9, 127.9, 125.1, 124.6, 123.7, 123.1, 120.6, 112.1, 48.2, 22.0. IR (film) ν_{max}: 3052, 2977, 2933, 1654, 1624, 1596, 1564, 1462, 1383, 1321 cm^{-1}. HR-MS (ESI) m/z: calcd for $C_{20}H_{20}N_3O$ $[M+H]^+$: 318.1606; found 318.1603. HPLC purity 95.0% (30 min run of 45-80% CH_3CN in H_2O, with 15 min gradient, 1.0 mL/min).

4.4 Cell culture

All cell lines were initially purchased from American Type Culture Collection (ATCC). The PC-3 and LNCaP prostate cancer cell lines were routinely cultured in RPMI-1640 medium supplemented with 10% FBS and 1% penicillin/streptomycin. Cultures were maintained in a high humidity environment supplemented with 5% carbon dioxide at a temperature of 37^{o}C. The DU-145 prostate cancer cells were routinely cultured in Eagle's Minimum Essential Medium (EMEM) supplemented with 10% FBS and 1% penicillin/ streptomycin. LNCaP95, VCaP, and 22Rv1 cells were maintained in Dr. Yan Dong's laboratory at Tulane School of Medicine and have been previously characterized [18,19].

4.5 WST-1 cell proliferation assay

PC-3, DU-145, or LNCaP were plated in 96-well plates at a density of 3,200 each well in 200 µL of culture medium. PWR-1E was plated in 96-well plates at a density of 5,000 each well in 200 µL of culture medium. The cells were then treated with curcumin, or synthesized analogues separately at different doses for 3 days, while equal treatment volumes of DMSO were used as vehicle control. The cells were cultured in a CO_2 incubator at 37 ^{o}C for three days. 10 µL of the premixed WST-1 cell proliferation reagent (Clontech) was added to each well. After mixing gently for one minute on an orbital shaker, the cells were incubated for additional 3 hours at 37 ^{o}C. To ensure homogeneous distribution of color, it is important to mix gently on an orbital shaker for one minute. The absorbance of each well was measured using a microplate-reader (Synergy HT, BioTek) at a wavelength of 430

nm. The IC_{50} value is the concentration of each compound that inhibits cell proliferation by 50% under the experimental conditions and is the average from triplicate determinations that were reproducible and statistically significant. For calculating the IC_{50} values, a linear proliferative inhibition was made based on at least five dosages for each compound.

4.6 Cell cycle analysis

PC-3 cells were plated in 24-well plates at a density of 200,000 each well in 400 µL of culture medium. After 3 h of cell attachment, the cells were then treated with dienone **28** at 5 µM and dienone **46** at 4 µM, while equal treatment volumes of DMSO were used as vehicle control. The cells were cultured in CO_2 incubator at 37 ^oC for 16 h. Both attached and floating cells were collected in a centrifuge tube by centrifugation at rcf 450 g for 5 min. After discarding the supernatant, the collected cells were re-suspended with 500 µL 80% cold ethanol to fix for 30 min in 4 ^oC. The fixed cells could be stored at -20 ^oC for one week. After fixation, the ethanol was removed after centrifuging and the cells were washed with PBS. The cells were then re-suspended with 100 µL of 100 mg/mL ribonuclease and were cultured at 37 ^oC for 30 min to degrade all RNA. The cells were stained with 200 µL of 50 µg/mL propidium iodide (PI) stock solution for 30 min at -20 ^oC, and then the fluorescence intensity of PI was detected in individual PC-3 cells using an Attune flow cytometer (Life Technologies) within 0.5-1 h after staining.

4.7 F2N12S and CYTOX AADvanced double staining assay

PC-3 cells were plated in 24-well plates at a density of 200,000 each well in 400 µL of culture medium. After 3 h of cell attachment, the cells were then treated with the test compound at different concentrations and cultured in CO_2 incubator at 37 ^oC for 16 h, while equal treatment volumes of DMSO were used as vehicle control. Both attached and floating cells were collected in a centrifuge tube by centrifugation at rcf value of 450 g for 5 min. The collected cells were re-suspended with 500 µL HBSS to remove proteins which may affect flow signal and centrifuged again. After discarding the supernatant, the collected cells were re-suspended with 300 µL HBSS and stained with 0.3 µL of F2N12S for 3-5 min followed by 0.3 µL SYTOX AADvanced for an additional 5 min. The fluorescence intensity of the two probes was further measured in individual PC-3 cells using an Attune flow cytometer (Life Technologies) within 0.5-1 h after staining.

4.8 Pharmacokinetic Study (Sampling and Analysis) [23]

Male Sprague-Dawley rats, weighing between 250 and 300 g (Charles River Laboratories, Portage, MI) were used for the pharmacokinetic study of compounds **28**, **46**, **49**, and **58**. Rats (n = 4) were given oral gavage containing 5% dimethyl sulfoxide (DMSO), 40% polyethylene glycol 400, 55% saline-dissolved **28**, **46**, **49**, and **58** at a single dose of 10 mg/kg. After oral administration, blood samples were collected from the lateral tail vein of the rats at 1, 3, 6, and 24 h. Rat blood was collected with a capillary into 1.5 mL microcentrifuge tubes containing 0.01 mL of 10% EDTA anticoagulant. Plasma was then separated from red cells by centrifugation in a refrigerated centrifuge at 4 °C and transferred to a separate tube. The plasma samples were frozen at −80 °C until analysis. All procedures involving these animals were conducted in compliance with state and federal laws, standards of the U.S. Department of Health and Human Services, and guidelines established by Xavier University Animal Care and Use Committee. The facilities and laboratory animals program of Xavier University are accredited by the Association for the Assessment and Accreditation of Laboratory Animal Care.

4.9 High Performance Liquid Chromatography−Tandem Mass Spectrometry (HPLC−MS/MS) for Drug Analysis in Plasma Samples

Plasma samples were extracted with chloroform/methanol (2:1) using traditional Folch method for lipid extraction. Methanol (1mL) and chloroform (2 mL) were added to each plasma sample followed by addition of 5 ng of trans-tamoxifen-$^{13}C2,^{15}N$ to each sample as the internal standard. The mixtures were stored at −20 °C overnight. Next the samples were sonicated for 5 min and centrifuged with a Thermo Scientific Heraeus Megafuge16 centrifuge. The top layer was transferred to another test tube. The bottom layer was washed with 1 mL of chloroform/methanol (2:1), centrifuged, and the top layer was transferred and combined with the previous top layer. Eight-tenth of a milliliter of HPLC grade water was added to the extracts. After vortexing, the mixture was centrifuged. The bottom layer was dried out with nitrogen and re-suspended in 100 μL of HPLC grade acetonitrile. An aliquot of 10 μL of sample was injected onto a Hypersil Gold column (50 mm × 2.1 mm; particle size 1.9 μm, Thermo Scientific) on a Dionex Ultimate 3000 UPLC system equipped with a TSQ Vantage triple quadrupole mass spectrometer for analysis. A binary mobile phase (A, water with 0.05% formic acid; B, acetonitrile with 0.05% formic acid) was used to achieve the gradient of initial 30% B for 1 min and then to 80% B at 8 min, to 100% B at 9 min, and returned to 30% B for 4 min. The flow rate was controlled at 0.6 mL/min. The settings of HESI source were as follows: spray voltage (3200 V); vaporizer temperature (365 °C); sheath gas pressure (45 psi); auxiliary gas pressure (10 psi); capillary

temperature (330 °C). Nitrogen was used as the sheath gas and auxiliary gas. Argon was used as the collision gas.

*4.10 . Incubation of compound **28** (or **49**) with rat liver microsomes (Total 300 µL)*

The pre-incubation solution was prepared by adding 30 µL of potassium phosphate buffer (pH 7.4; 10X), 241.5 µL water, 15 µL of NADPH solution A, 3µL of NADPH solution B, 7.5 µL pooled human liver microsomes from Corning Gentest into a 1.5 mL microcentrifuge. The mixtures were incubated at 37 °C for 5 min in an incubator. Then 3 µL of 10 mM **28** (or **49**) was added, mixed, and incubated at 37 °C for 60 min in the incubator. After incubation, 300 µL MeOH was added to terminate the reaction. The final mixture was then centrifuged at 10,000 × g for 4 min at 4 °C. The supernatant was analyzed on a high resolution mass spectrometer Q-Exactive from Thermo Fisher Scientific connected with a UHPLC ultimate 3000 from Dionex.

4.11 Statistical analysis

All data are represented as the mean ± standard deviation (S.D.) for the number of experiments indicated. Other differences between treated and control groups were analyzed using the Student's t-test. A p-value < 0.05 was considered statistically significant.

ACKNOWLEDGMENT

This work was financially supported by California State University (CSU)-Fresno and CSU Program for Education and Research in Biotechnology (CSUPERB) 2013 New Investigator and 2015 Research Development Award. The *in vivo* Pharmacokinetic Studies, Metabolic Profile Studies, and HRMS were supported by NIH RCMI program at Xavier University of Louisiana through Grant 2G12MD007595-064 (G. Wang). N.S. was supported in part by an S-STEM Graduate Student Scholarship from National Science Foundation (Award #: 1059994). We are also grateful to the Graduate Net Initiative at CSU-Fresno for Graduate Research Fellowships (to X.Z. and M.P.), to the Division of Graduate Studies at CSU-Fresno for a Graduate Student Research and Creative Activities Support Award (to M.P), and to the Undergraduate Studies at CSU-Fresno for Undergraduate Research Grants (to G.R.P. and J.K.).

Appendix A. Supplementary data.

Supplementary data related to this article can be found at http://.

REFERENCES

[1] S.C. Gupta, S. Prasad, J.H. Kin, S. Patchva, L.J. Webb, I.K. Priyadarsini, B.B. Aggarwal, Multitargeting by curcumin as revealed by molecular interaction studies, Nat. Prod. Rep. 28 (2011) 1937-1955.

[2] T. Dorai, N. Gehani, A. Katz, Therapeutic potential of curcumin in human prostate cancer. I. Curcumin induces apoptosis in both androgen-dependent and androgen-independent prostate cancer cells, Prostate Cancer Prostatic Dis. 3 (2000) 84-93.

[3] Q.-H. Chen, Curcumin-based anti-prostate cancer agents, Anti-Cancer Agents Med. Chem. 15 (2015) 138-156.

[4] M.-H. Teiten, F. Gaascht, S. Eifes, M. Dicato, M. Diederich, Chemopreventive potential of curcumin in prostate cancer. Genes Nutr. 5 (2010) 61-74.

[5] D. Shetty, Y.J. Kim, H. Shim, J.P. Snyder, Eliminating the heart from the curcumin molecule: Monocarbonyl curcumin mimics. Molecules 20 (2015) 249-292.

[6] N. Samaan, Q. Zhong, J. Fermandez, G. Chen, A.M. Hussain, S. Zheng, G. Wang, Q.-H. Chen, Design, synthesis, and evaluation of novel heteroaromatic analogs of curcumin as anti-cancer agents, Eur. J. Med. Chem. 75 (2014) 123-131.

[7] R. Wang, C. Chen, X. Zhang, C. Zhang, Q. Zhong, G. Chen, Q. Zhang, S. Zhang, G. Wang, Q.-H. Chen, Structure-activity relationship and pharmacokinetic studies of 1,5-diheteroarylpenta-1,4-dien-3-ones: a class of promising curcumin-based anti-cancer agents. J. Med. Chem. 58 (2015) 4713-4726.

[8] R. Wang, X. Zhang, C. Chen, G. Chen,; Q. Zhong, Q. Zhang, S. Zheng, G. Wang, Q.-H. Chen, Synthesis and evaluation of 1,7-diheteroarylhepta-1,4,6-trien-3-ones as curcumin-based anticancer agents, Eur. J. Med. Chem. 110 (2016) 164-180.

[9] X. Zhang, R. Wang, G.R. Perez, G. Chen, Q. Zhang, S. Zheng, G. Wang, Q.-H. Chen, Design, synthesis, and biological evaluation of 1,9-diheteroarylnona-1,3,6,8-tetraen-5-ones as a new class of anti-prostate cancer agents, Bioorg. Med. Chem. 24 (2016) 4692-4700.

[10] M.F.F.M. Aluwi, K. Rullah, B.M. Yamin, S.W. Leong, M.N.A. Bahari, S.J. Lim, S.M.M. Faudzi, J. Jalil, F. Abas, N.M. Fauzi, N.H. Ismail, I. Jantan, K.K. Lam, Bioorg. Med. Chem. Lett. 26 (2016) 2531-2538.

[11] Q. Li, J. Chen, S. Luo, J. Xu, Q. Huang, Synthesis and assessment of the antioxidant and antitumor properties of asymmetric curcumin analogues, Eur. J. Med. Chem. 93 (2015) 461-469.

[12] M. Seto, N. Miyamoto, K. Aikawa, Y. Aramaki, N. Kanzaki, Y. Lizawa, M. Baba, M. Shiraishi, Orally active CCR5 antagonists as anti-HIV-1 agents. Part 3: synthesis and biological activities of 1-benzazepine derivatives containing a sulfoxide moiety, Bioorg. Med. Chem. 13 (2005) 363-386.

[13] M.M. Webber, D. Bello, H.K. Kleinman, D.D. Wartinger, D.E. Williams, J.S. Rhim, Prostate specific antigen and androgen receptor induction and characterization of an immortalized adult human prostatic epithelial cell line, Carcinogenesis 17 (1996) 1641-1646.

[14] S.C. Gupta, S. Patchva, W. Koh, B.B Aggarwal, Discovery of curcumin, a component of golden spice, and its miraculous biological activities, Clin. Exp. Pharmacol. Physiol. 39 (2012) 283-299.

[15] T. Shankar, N. Shantha, H. Ramesh, I. Murthy, V. Murthy, Toxicity studies on turmeric (*Curcuma longa*): acute toxicity in rats, guinepigs & monkeys, Indian J. Exp. Biol. 18 (1980**)** 73-75.

[16] S.R. Denmeade, X.S. Lin, J.T. Isaacs, Role of programmed (apoptotic) cell death during the progression and therapy for prostate cancer, Prostate (N.Y.) 28 (1996) 251-265.

[17] K.H. Tsui, T.H. Feng, C.M. Lin, P.L. Chang, H.H. Juang, Curcumin blocks the activation of androgen and interlukin-6 on prostate-specific antigen in human prostateic carcinoma cells, J. Androl. 29 (2008) 661-668.

[18] B. Cao, Y. Qi, G. Zhang, D. Xu, Y. Zhan, X. Alvarez, Z. Guo, X. Fu, S.R. Plymate, O. Sartor, H. Zhang, Y. Dong, Androgen receptor splice variants activating the full-length receptor in mediating resistance to androgen-directed therapy, Oncotarget. 30 (2014) 1646-1656.

[19] L.L. Liu, N. Xie, S. Sun, S. Plymate, E. Mostaghel, X. Dong, Mechanisms of the androgen receptor splicing in prostate cancer cells, Oncogene 12 (2014**)** 3140-3150.

[20] R.K. Srivastava, Q. Chen, I. Siddiqui, K. Sarva, S. Shankar, Linkage of curcumin-induced cell cycle arrest and apoptosis by cyclin-dependent kinase inhibitor p21/WAF1/CIP1, Cell Cycle, 6 (2007) 2953-2961.

[21] W. Wichitnithad, U. Nimmannit, S. Wacharasindhu, P. Rojsitthisak, Synthesis, characterization and biological evaluation of succinate prodrugs of curcuminoids for colon cancer treatment, Molecules 16 (2011) 1888–1900.

[22] B. Corbel, L. Medinger, J.P. Haelters, G. Sturtz, An efficient synthesis of dialkyl 2-oxoalkanephosphonates and diphenyl-2-oxoalkylphosphine oxides from 1-chloralkyl ketones, Synthesis (1985) 1048–1051.

[23] Y.-Z. Lee, C.-W. Yang, H.-Y. Hsu, Y.-Q. Qiu, T.-K. Yeh, H.-Y. Chang, Y.-S. Chao, S.-J. Lee, Synthesis and biological evaluation of tylophorine-derived dibenzoquinolines as orally active agents: exploration of the role of tylophorine E ring on biological activity, J. Med. Chem. 55 (2012) 10363−10377.

Highlights:

- 34 New asymmetric dienones were evaluated in prostate epithelial cell models.
- The asymmetric dienones are more potent than the corresponding symmetric ones.
- The optimal trienone is 219- to 636-fold more potent than curcumin.
- Two promising compounds exhibit improved potency and bioavailability.
- Four dienones show cytotoxicity in enzalutamide-resistant prostate cancer cells.